This is the accepted manuscript (postprint) of the following article:
A. Parvinnasab, S. Rostami, A. Namdar, E. Salahinejad, A.H. Taghvaei, S. Abdi, S. Rajabi, L. Tayebi, *Balanced enhancement of antibacterial activity and biocompatibility in chitosan-vancomycin 3D-printed scaffolds through mesoporous bioactive glass addition*, Journal of Drug Delivery Science and Technology, 105 (2025) 106637.
https://doi.org/10.1016/j.jddst.2025.106637

Balanced enhancement of antibacterial activity and biocompatibility in chitosan-vancomycin 3D-printed scaffolds through mesoporous bioactive glass addition

Amir Parvinnasab [a], Sahar Rostami [a], Ashkan Namdar [a], Erfan Salahinejad [a,*], Amir Hossein Taghvaei [b], Shaghayegh Abdi [c], Sarah Rajabi [c,d], Lobat Tayebi [e,f]

[a] *Faculty of Materials Science and Engineering, K. N. Toosi University of Technology, Tehran, Iran*

[b] *Department of Materials Science and Engineering, Shiraz University of Technology, Shiraz, Iran*

[c] *Department of Cell Engineering, Cell Science Research Center, Royan Institute for Stem Cell Biology and Technology, ACECR, Tehran, Iran*

[d] *Department of Tissue Engineering, School of Advanced Technologies in Medicine, Royan Institute, Tehran, Iran.*

[e] *Marquette University School of Dentistry, Milwaukee, WI 53233, USA*

f Institute for Engineering in Medicine, Health, & Human Performance (EnMed), Batten College of Engineering and Technology, Old Dominion University, Norfolk, VA 23529, USA

Abstract

The rising incidence of osteomyelitis and growing challenges associated with conventional antibiotic therapy underscore an urgent need for novel therapeutic interventions. This study explores the development and characterization of chitosan/vancomycin/mesoporous bioactive

* Corresponding author: Email Address: <salahinejad@kntu.ac.ir>

This is the accepted manuscript (postprint) of the following article:
A. Parvinnasab, S. Rostami, A. Namdar, E. Salahinejad, A.H. Taghvaei, S. Abdi, S. Rajabi, L. Tayebi, *Balanced enhancement of antibacterial activity and biocompatibility in chitosan-vancomycin 3D-printed scaffolds through mesoporous bioactive glass addition*, Journal of Drug Delivery Science and Technology, 105 (2025) 106637.
https://doi.org/10.1016/j.jddst.2025.106637

glass (Chi-Van-MBG) 3D-printed scaffolds incorporating various MBG/Chi ratios, aimed at enhancing the viability and proliferation of human bone marrow mesenchymal stem cells (hBMSCs) along with antibacterial effectiveness. Preliminary analyses, including the assessment of chemical composition, morphology, swelling, and degradation behaviors, demonstrated promising characteristics for bone tissue engineering applications. The scaffolds also exhibited an initial burst release of vancomycin, followed by a sustained release over four weeks, ensuring effective antibacterial potency. Notably, a considerable inhibition zone of 40 mm against *Staphylococcus aureus* was found for the composite sample loaded with 15% MBG, compared to 24 mm for the drug-loaded, MBG-free sample during antibacterial disk diffusion assays. Furthermore, MTS assays indicated a remarkable cell viability of 191.2 % for the optimal specimen (the sample with 10% MBG) after 7 days of culture. Cell adhesion investigations revealed a bridging framework that facilitates both single-cell and multi-cell attachments due to the structural features of the optimal 3D-printed scaffold. Overall, the Chi-Van-MBG scaffolds represent promising biomaterials for addressing osteomyelitis, harmonizing enhanced antibacterial properties with exceptional biocompatibility and favorable cellular responses.

Keywords: *3D printing; Tissue regeneration; Biocompatibility; Bacterial infection; Biofilm*

1. Introduction

Chitosan is a biopolymer derived from natural sources, specifically chitin, characterized by a linear arrangement of (1-4) glycosidic bonds that connect d-glucoasmine units, with a varying proportion of N-acetyl d-glucosamine groups distributed randomly. Its desirable biocompatibility

This is the accepted manuscript (postprint) of the following article:
A. Parvinnasab, S. Rostami, A. Namdar, E. Salahinejad, A.H. Taghvaei, S. Abdi, S. Rajabi, L. Tayebi, *Balanced enhancement of antibacterial activity and biocompatibility in chitosan-vancomycin 3D-printed scaffolds through mesoporous bioactive glass addition*, Journal of Drug Delivery Science and Technology, 105 (2025) 106637.
https://doi.org/10.1016/j.jddst.2025.106637

and biodegradability have made it promising for diverse biomedical applications. Specifically, chitosan supports the proliferation of bone-forming osteoblast cells, and exhibits a level of bioactivity and osteoconductivity [1,2], highlighting its potential for bone tissue engineering applications. Despite its benefits, chitosan has some drawbacks that challenge its use in bone regenerative engineering. Its bioactivity is not high enough to ensure effective attachment to the surrounding bone tissue [3]. It also lacks necessary mechanical properties for use in load-bearing applications [4]. Another disadvantage of chitosan is that despite having a level of antibacterial properties [5,6], its activity is not sufficient to eradicate most bacterial threats and is highly dependent on its structural and environmental conditions [7,8]. Therefore, the formation of biofilms is a significant concern when using chitosan, as it can significantly compromise its efficacy in biomedical applications.

In bone substitution practices, a common infection known as osteomyelitis can cause severe implications for patients. This infectious disease mainly occurs in response to the bacterial activity of *Staphylococcus aureus (S. aureus)*. This gram-positive bacterium can be mostly eradicated using vancomycin, a glycopeptide antibiotic [9,10]. The incorporation of vancomycin into chitosan has been shown to successfully eradicate *S. aureus* biofilms [11–14]; however, the potential adverse effects of vancomycin remain a concern. It has been established that daily vancomycin concentrations above 80 µg/mL can cause permanent, irreversible damage to the body [15]. Another study indicated that the systematic administration of vancomycin at a mean level of 27.5 µg/mL per day can leads to nephrotoxicity in patients [16]. An evidence-based meta-analysis reported that the localized administration of vancomycin up to 1.5 mg/ml carries a limited risk of

This is the accepted manuscript (postprint) of the following article:
A. Parvinnasab, S. Rostami, A. Namdar, E. Salahinejad, A.H. Taghvaei, S. Abdi, S. Rajabi, L. Tayebi, *Balanced enhancement of antibacterial activity and biocompatibility in chitosan-vancomycin 3D-printed scaffolds through mesoporous bioactive glass addition*, Journal of Drug Delivery Science and Technology, 105 (2025) 106637.
https://doi.org/10.1016/j.jddst.2025.106637

toxicity, provided that it does not enter the bloodstream. However, challenges arise when localized serum is transferred to the blood, mimicking a semi-systematic administration of vancomycin and introducing associated risks [17]. Additionally, unmonitored localized vancomycin administration may lead to a condition known as vancomycin flushing syndrome (or red man syndrome), a hypersensitivity allergic reaction to vancomycin [18,19]. Although optimizing the loading amount and release kinetics of the medication can potentially address these issues, controlling these two factors may be challenging or insufficient in conditions where a bacterial biofilm has formed and/or higher doses are required. As well as viability, vancomycin can limit other key cell activities, such as attachment, proliferation, migration, and differentiation, diminishing or avoiding the scaffold's regenerative effectiveness [20,21]. Therefore, balancing the scaffold's antimicrobial properties while maintaining or enhancing cell functions is vital for optimal performance.

One possible approach to compensate for the adverse effects of inevitably loaded factors, such as antibiotics, is to include agents that promote cellular activities. Typically, the release of certain ions, such as Ca^{2+}, Mg^{2+}, Si^{4+}, Ba^{2+}, Sr^{2+}, Cu^{2+}, PO_4^{3-}, F^-, etc, into the body can fulfill this role [22,23]. A well-documented category of biomaterials that are known to provide such properties is bioactive glasses and glass-ceramics. Features like osteoconductivity and osteoinductivity along with reliable mechanical properties are also achievable through the incorporation of these bioceramics into polymer-matrix composites [24,25]. Typically, Pishbin *et al.* [26] developed chitosan/bioactive glass/nano-silver coatings on AISI 316L stainless steel and evaluated the impact of bioactive glass additions. They observed that over a 7-day period, the non-impregnated chitosan coating promoted the viability of osteoblast-like MG-63 to approximately

This is the accepted manuscript (postprint) of the following article:
A. Parvinnasab, S. Rostami, A. Namdar, E. Salahinejad, A.H. Taghvaei, S. Abdi, S. Rajabi, L. Tayebi, *Balanced enhancement of antibacterial activity and biocompatibility in chitosan-vancomycin 3D-printed scaffolds through mesoporous bioactive glass addition*, Journal of Drug Delivery Science and Technology, 105 (2025) 106637.
https://doi.org/10.1016/j.jddst.2025.106637

145%, while the chitosan/bioactive glass coating achieved around 175% viability. Another study indicated that in hydroxypropylmethyl cellulose cross-linked chitosan scaffolds containing ZnO and bioactive glass, cell viability increased by up to 50% with the addition of bioactive glass compared to the bioactive glass-free scaffolds [27]. Also, El-Kady *et al.* [28] focused on vancomycin- and bioactive glass-incorporated chitosan-based scaffolds. They showed the BJ1 skin fibroblast cell survival of 94.3% for the chitosan-vancomycin scaffolds, whereas 25 and 50% bioactive glass addition led to the cell viabilities of 97.6 and 98.8%, respectively. Despite the improvements observed in the biocompatibility of vancomycin-loaded constructs using bioactive glasses, these enhancements are mostly insufficient to considerably mitigate the detrimental effects of vancomycin or to achieve a notable increase in cellular functions.

Mesoporous bioactive glasses (MBGs) exhibit superior porosity, surface area, and ion release rate compared to conventional counterparts [29–31]. These characteristics promote cell activity by creating a favorable environment for cellular functions such as attachment, proliferation, differentiation, and migration through their bioactive properties, structural features, and ion release mechanisms [32–35]. Additionally, the inherent antibacterial properties of MBGs, resulting from an increased ion release rate that creates an alkaline microenvironment [36–39], can reduce the amount of antibiotics required to achieve a desired therapeutic effect. Consequently, MBGs have promise in enhancing the interplay of antibacterial activity and biocompatibility in vancomycin-loaded chitosan constructs, as evidenced by the remarkable performance of MBG-loaded delivery systems with antibiotics loaded into polymeric matrices [40–42]. Regarding the chitosan/MBG/vancomycin system, there are only a few reports on

This is the accepted manuscript (postprint) of the following article:
A. Parvinnasab, S. Rostami, A. Namdar, E. Salahinejad, A.H. Taghvaei, S. Abdi, S. Rajabi, L. Tayebi, *Balanced enhancement of antibacterial activity and biocompatibility in chitosan-vancomycin 3D-printed scaffolds through mesoporous bioactive glass addition*, Journal of Drug Delivery Science and Technology, 105 (2025) 106637.
https://doi.org/10.1016/j.jddst.2025.106637

chitosan/hydroxyapatite/vancomycin-loaded MBG coatings applied on titanium [42,43]. Their results indicate that cell cytocompatibility decreases as the ratio of vancomycin-loaded MBG to hydroxyapatite increases. However, these studies did not explore how MBG moderates the toxic effect of vancomycin, since the vancomycin-to-MBG ratio was kept constant across all the samples. Also, the antibacterial activity of the samples at various levels of the constitutes was not analyzed, which would provide insight into the balance between biocompatibility and antibacterial efficacy. Additionally, to the best of our knowledge, there are no reports on the development of chitosan/MBG/vancomycin composites other than coatings. To address these research gaps, this study originally focuses on the cell biocompatibility and antibacterial responses of chitosan/MBG/vancomycin scaffolds fabricated through 3D printing with varying amounts of MBG incorporation at a fixed content of vancomycin loading. Reasons for selecting 3D printing include its precise customization, controlled porosity and pore size, reduced manufacturing time and cost, scalability, and reproducibility, making it an ideal method for manufacturing bone tissue engineering scaffolds. The hypothesis is that optimizing the incorporation level of MBG into chitosan impregnated with vancomycin will enhance both antibacterial activity and biocompatibility in a 3D-printed porous bone tissue engineering construct.

This is the accepted manuscript (postprint) of the following article:
A. Parvinnasab, S. Rostami, A. Namdar, E. Salahinejad, A.H. Taghvaei, S. Abdi, S. Rajabi, L. Tayebi, *Balanced enhancement of antibacterial activity and biocompatibility in chitosan-vancomycin 3D-printed scaffolds through mesoporous bioactive glass addition*, Journal of Drug Delivery Science and Technology, 105 (2025) 106637.
https://doi.org/10.1016/j.jddst.2025.106637

2. Materials and methods

2.1. Materials

Chitosan (deacetylation degree: 84.2%, molecular weight: 140469 g/mol), acetic acid (CH_3COOH, 100%), potassium hydroxide (KOH, 85.0%), hexadecyltrimethylammonium bromide (CTAB, $C_{19}H_{42}BrN$, >96.0%), glutaraldehyde ($OHC(CH_2)_3CHO$, 25% aqueous solution, ≥98%), and aqueous ammonia (NH_4OH, 28.0%) were obtained from Sigma-Aldrich, Germany. Ethyl acetate ($C_4H_8O_2$, 99.8%), tetraethylortosilicate (TEOS, $SiC_8H_{20}O_4$, 99.5%), calcium nitrate tetrahydrate ($CaNO_3.4H_2O$, 99.5%), and ethanol (C_2H_5OH, 96.0%) were also purchased from VWR chemicals. Vancomycin hydrochloride ($C_{66}H_{75}Cl_2N_9O_{24}.HCl$, 85.0%) was obtained from Thermo Fisher Scientific. 3-(4,5-dimethylthiazol-2-yl)-5-(3-carboxymethoxyphenyl)-2-(4-sulfophenyl)-2H-tetrazolium (MTS, CellTiter 96® AQ_{ueous}, Promega), fetal bovine serum (FBS, Gibco) and dulbecco's modified Eagle medium (DMEM, Sigma) were utilized for cell viability tests.

2.2. Synthesis of MBG

To synthesize MBG particles, the protocol described in Ref. [37] was followed. Briefly, 0.7 g CTAB was added to 33 mL deionized water, while being stirred for 1 h. Then, 10 ml ethyl acetate was introduced for the formation of microemulsion. After 30 min of stirring, 0.47 ammonium solution was poured into the container and stirred for another 15 min. 3.6 mL TEOS and 2.56 g calcium nitrate tetrahydrate were then added in the container in 30-min intervals and stirred for 4

This is the accepted manuscript (postprint) of the following article:
A. Parvinnasab, S. Rostami, A. Namdar, E. Salahinejad, A.H. Taghvaei, S. Abdi, S. Rajabi, L. Tayebi, *Balanced enhancement of antibacterial activity and biocompatibility in chitosan-vancomycin 3D-printed scaffolds through mesoporous bioactive glass addition*, Journal of Drug Delivery Science and Technology, 105 (2025) 106637.
https://doi.org/10.1016/j.jddst.2025.106637

h, giving white colloidal particles. The particles were extracted from by centrifuging, rinsed several times with water, and then dried at 60 ℃ overnight. Finally, the obtained powder was calcinated at 600 ℃ for 6 h, giving a binary-oxide composition of 86 mol% (84 wt%) SiO_2-14 mol% (16 wt%) CaO with the mean spherical particle size of 100 nm and the mean pore size of 3 nm [37].

2.3. Fabrication of scaffolds

3D-printing inks were prepared by dissolving 9.5 % w/v chitosan in a 2% v/v acetic acid solution at room temperature for 2 h. Vancomycin and MBG were then added to the chitosan solution with levels listed in Table 1 and continuously mixed under magnetic stirring for 2 h. The loading amount of the drug was extracted from previous studies on chitosan-based vancomycin-loaded constructs, ensuring effective antibacterial effects against *S. aureus* strains and acceptable biocompatibility [44,45].

Table 1. Specification of the 3D-printing inks

Sample names	Chitosan (% w/v)	Vancomycin (wt%)	MBG (wt%)
Chi	9.5	-	-
Chi-Van	9.5	8	-
Chi-Van-5MBG	9.5	8	5
Chi-Van-10MBG	9.5	8	10
Chi-Van-15MBG	9.5	8	15

This is the accepted manuscript (postprint) of the following article:
A. Parvinnasab, S. Rostami, A. Namdar, E. Salahinejad, A.H. Taghvaei, S. Abdi, S. Rajabi, L. Tayebi, *Balanced enhancement of antibacterial activity and biocompatibility in chitosan-vancomycin 3D-printed scaffolds through mesoporous bioactive glass addition*, Journal of Drug Delivery Science and Technology, 105 (2025) 106637.
https://doi.org/10.1016/j.jddst.2025.106637

The prepared inks were transferred into a stainless-steel cartridge syringe equipped with a nozzle of gauge 24G having an inner diameter of 0.3 mm. Scaffolds of two printed layers with the dimensions of 2×2×0.13 cm^2 and pore sizes ranging within 150-300 μm were successfully deposited on a glass sheet at room temperature using a liquid deposition modeling 3D printer with the flow rate of 200 mm^3/min and the feed rate of 150 mm/min. The fabricated scaffolds were then modified in a 1.5 M KOH solution at 4 ℃ for 10 min, washing with water and ethanol, and freeze-drying to remove remaining volatile residuals.

2.4. Characterization

2.4.1. Structure

Scanning electron microscopy (SEM, Tescan, MIRA3) was utilized to validate the morphology of the 3D-printed constructs at an accelerating voltage of 20 kV after being coated with a 20 μm-thick gold layer. Functional groups in the samples were also explored by attenuated total reflectance-Fourier transform infrared spectroscopy (ATR-FTIR, Bruker Tensor 27 spectrometer, Germany) within 4000-400 cm^{-1} wavenumber with a resolution of 4 cm^{-1} and an average scan number of 32.

2.4.2. Degradability

The two-layered scaffolds of 1×1×0.13 cm^3 with an initial weight W_i were soaked in 25 mL phosphate-buffered saline (PBS). At specific timeframes, the samples were carefully removed,

This is the accepted manuscript (postprint) of the following article:
A. Parvinnasab, S. Rostami, A. Namdar, E. Salahinejad, A.H. Taghvaei, S. Abdi, S. Rajabi, L. Tayebi, *Balanced enhancement of antibacterial activity and biocompatibility in chitosan-vancomycin 3D-printed scaffolds through mesoporous bioactive glass addition*, Journal of Drug Delivery Science and Technology, 105 (2025) 106637.
https://doi.org/10.1016/j.jddst.2025.106637

rinsed with water, dried at 50 °C for 2 h, and weighed to obtain the final dry weight W_f. The degradation degree was calculated using this formula:

$$Degradation\ degree\ = \frac{(W_i - W_f)}{W_i} \times 100 \quad \text{(Eq. 1)}$$

2.4.3. Swelling capability

In order to determine the water uptake capability of the scaffolds, the two-layered samples of 1×1×0.13 cm^3, weighted at W_i, and immersed in 25 mL PBS at 37 °C. At predetermined time intervals, the swollen samples were carefully removed, gently placed on a filter paper to remove any excess surface liquid, and weighed again (W_{wet}). The swelling degree was calculated using the fallowing formula:

$$Swelling\ degree = \frac{W_{wet} - W_i}{W_i} \times 100 \quad \text{(Eq. 2)}$$

2.4.4. Drug delivery

To determine the release kinetics of vancomycin from the two-layered samples of 0.25×0.25×0.13 cm^3, the concentration of the medication was measured in predetermined time intervals after soaking them inside 3 mL PBS. For such purpose, UV spectroscopy (Bloor Azma) was utilized at a wavelength of 280 nm after plotting a regression calibration curve with different dilutions of vancomycin.

This is the accepted manuscript (postprint) of the following article:
A. Parvinnasab, S. Rostami, A. Namdar, E. Salahinejad, A.H. Taghvaei, S. Abdi, S. Rajabi, L. Tayebi, *Balanced enhancement of antibacterial activity and biocompatibility in chitosan-vancomycin 3D-printed scaffolds through mesoporous bioactive glass addition*, Journal of Drug Delivery Science and Technology, 105 (2025) 106637.
https://doi.org/10.1016/j.jddst.2025.106637

2.4.5. Antimicrobial activity

The antibacterial efficiency of the fabricated scaffolds with respect to *S. aureus ATCC25923* bacterial strains was evaluated using the disk diffusion method. A density of 1.5×10^8 CFU/mL of bacteria strains was inoculated onto agar plates and incubated at 37 °C for 24 h. The $2\times2\times0.13$ cm^3 scaffolds were sterilized under UV-C for 2 h and then positioned onto the agar plates. The plates were incubated at 37 °C for 24 h, and bacterial inhibition zones around each sample was then measured using a digital caliper. Vancomycin antibiotic was used as the positive control and the PBS-smeared sterilized paper disk as the negative control.

2.4.6. Cytocompatibility and cell attachment

To assess the *in vitro* biocompatibility of the scaffolds, the MTS assay was conducted using human bone marrow-derived mesenchymal stem cells (hMSCs) at passages 4-6. The scaffolds were first sterilized with UV irradiation for 15 min and 70% ethanol for 5 h, followed by placing in a 96-well plate. A density of 1×10^4 cells/well were seeded on the samples, and after designated culture periods (1, 3, and 7 days) in 10% FBS-supplemented DMEM under standard cell culture conditions of 37 °C and 5% CO_2, the MTS solution was added to each well and allowed for the reduction of MTS by viable cells for 3 h. Following this incubation period, the formazan product was quantified by measuring the absorbance at 490 nm using a microplate reader (Thermo Scientific Multiskan Spectrum, MA, USA).

This is the accepted manuscript (postprint) of the following article:
A. Parvinnasab, S. Rostami, A. Namdar, E. Salahinejad, A.H. Taghvaei, S. Abdi, S. Rajabi, L. Tayebi, *Balanced enhancement of antibacterial activity and biocompatibility in chitosan-vancomycin 3D-printed scaffolds through mesoporous bioactive glass addition*, Journal of Drug Delivery Science and Technology, 105 (2025) 106637.
https://doi.org/10.1016/j.jddst.2025.106637

The optimal sample of the MTS assay was analyzed for cell attachment to further investigate cell-scaffold interactions. For this purpose, the sterilized 0.25×0.25×0.13 cm^3 scaffolds were seeded with hMSCs at 1×10^4 cells/cm^2 and cultured in DMEM supplemented with 10% FBS at 37°C and 5% CO_2. After 7 days, the samples were immersed in 2.5% v/v glutaraldehyde solution for 2 h to fix cells, followed by washing twice with PBS. Dehydration was also carried out by serially transferring the scaffolds through increasing ethanol concentrations (30, 50, 70, 90, 95, and 100%) for 10 min each. The scaffolds were dried for 12 h in room temperature and were coated with a gold layer for imaging with SEM at 20 kV.

2.4.7. Statistical analysis

All the experiments were conducted in triplicate, and the acquired data underwent rigorous statistical analysis via SPSS software. The differences between the samples were meticulously examined using one-way analysis of variance (ANOVA), succeeded by the application of the Tukey post hoc test, at significance levels set at $p < 0.05$, $p < 0.01$, and $p < 0.001$.

3. Results and discussion

3.1. Structure of the fabricated scaffolds

Fig. 1a-j depict the SEM images of the produced scaffolds, indicating the successful development of well-defined porous structures in all the samples. The mean pore and filament

This is the accepted manuscript (postprint) of the following article:
A. Parvinnasab, S. Rostami, A. Namdar, E. Salahinejad, A.H. Taghvaei, S. Abdi, S. Rajabi, L. Tayebi, *Balanced enhancement of antibacterial activity and biocompatibility in chitosan-vancomycin 3D-printed scaffolds through mesoporous bioactive glass addition*, Journal of Drug Delivery Science and Technology, 105 (2025) 106637.
https://doi.org/10.1016/j.jddst.2025.106637

sizes of the specimens, extracted from the SEM images, are also presented in Fig. 1k. The results show no significant differences among the samples (p-value > 0.05). It is well-established that pore sizes ranging within 75-300 μm are suitable for bone tissue engineering, as they facilitate the supply of oxygen and nutrients while allowing for the removal of waste, which is critical for cellular activity [46,47]. That is, the pore size of the scaffolds fabricated in this study falls within the appropriate range. It is also evident that increasing the MBG content causes the filaments to become rougher, which can be attributed local agglomeration of MBG particles, in agreement with the literature [48,49].

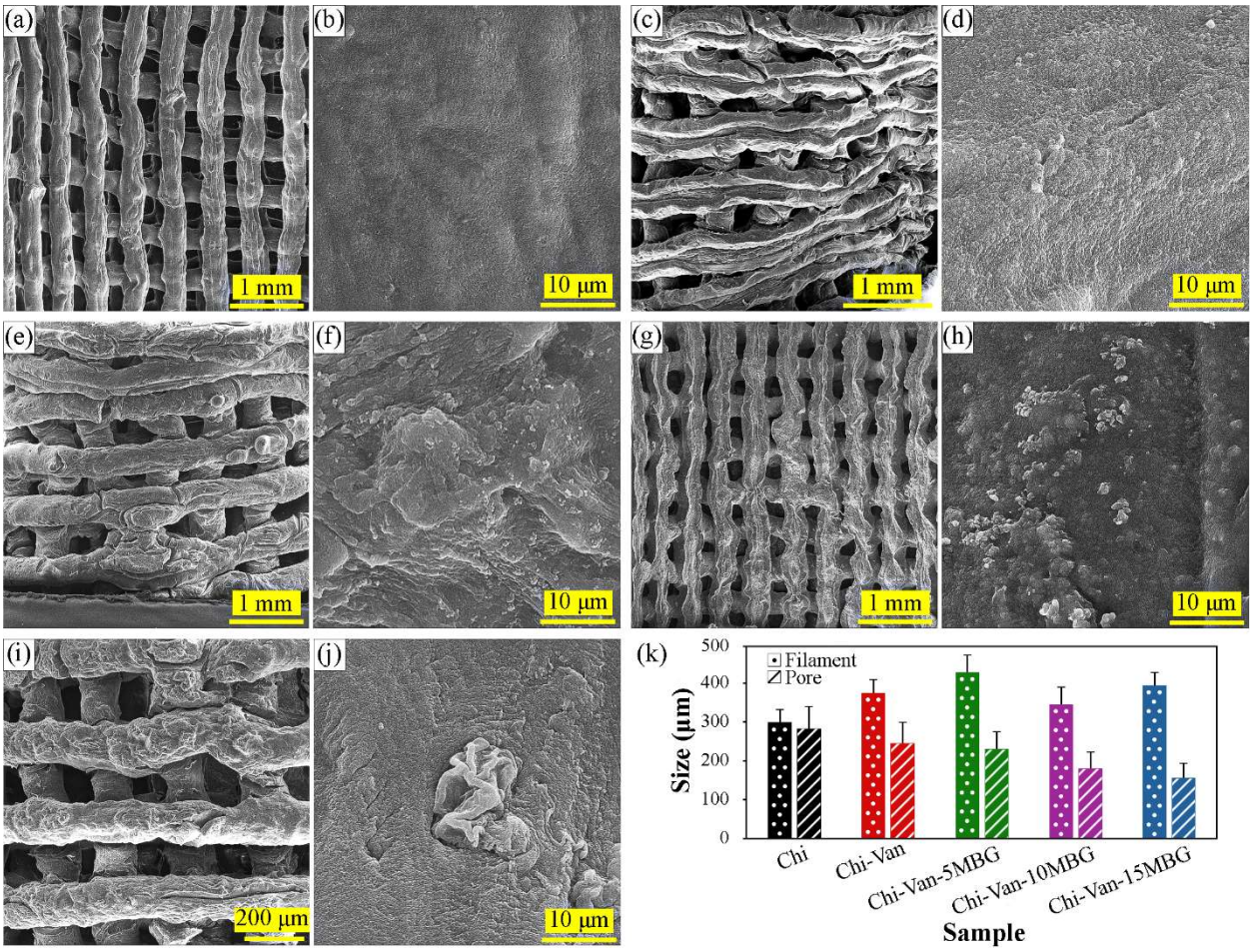

This is the accepted manuscript (postprint) of the following article:
A. Parvinnasab, S. Rostami, A. Namdar, E. Salahinejad, A.H. Taghvaei, S. Abdi, S. Rajabi, L. Tayebi, *Balanced enhancement of antibacterial activity and biocompatibility in chitosan-vancomycin 3D-printed scaffolds through mesoporous bioactive glass addition*, Journal of Drug Delivery Science and Technology, 105 (2025) 106637.
https://doi.org/10.1016/j.jddst.2025.106637

Fig. 1. SEM images of the Chi (a, b), Chi-Van (c, d), Chi-Van-5MBG (e, f), Chi-Van-10MBG (g, h), and Chi-Van-15MBG (i, j) scaffolds in different magnifications. Dimensions extracted from the SEM images (k), with No statistically significant differences between the samples ($p > 0.05$).

Fig. 2 illustrates the FTIR spectra of the scaffolds. Regarding the Chi scaffold, the peak located at 1026 cm^{-1} corresponds to the stretching vibrations of C–O bonds, while the peak around 1151 cm^{-1} is associated with C–O–C bonds in glycosidic linkages [50]. Furthermore, the peak at around 1376 cm^{-1} indicates the bending vibration of C–H bonds. The peak at around 1560 cm^{-1} corresponds to the bending vibrations of amid II (N–H) and stretching vibrations of C–N bonds, while the peak at 1646 cm^{-1} is related to the stretching vibrations of amid I (C=O) bonds of chitosan [51]. Peaks at 2850 and 2922 cm^{-1} are linked to the stretching vibrations of C–H bonds. The broad peak at 3351 cm^{-1} is also assigned to the stretching vibrations of amine and hydroxyl groups in chitosan [52]. Regarding Chi-Van, it is worth mentioning that vancomycin molecules contain methyl (CH_3) and methylene (CH_2) groups, giving rise to C–H bending modes [53]. A notable alteration compared to the Chi sample is observed in the range of 1300 to 1650 cm^{-1}. The increased intensity of the peaks at the lower values of this range can be attributed to the presence of phenolic hydroxyl groups due to the inclusion of vancomycin. The peak at 1646 cm^{-1} is related to the presence of C=O bonds, while the appearance of an absorbance peak at 1467 cm^{-1} is attributed to the presence of C=C bonds [54]. The peaks around 3351 cm^{-1} (corresponding to O–H and N–H) are less evident in the vancomycin-impregnated scaffolds, suggesting the hydrogen-bonding of these groups between vancomycin and chitosan [55].

This is the accepted manuscript (postprint) of the following article:
A. Parvinnasab, S. Rostami, A. Namdar, E. Salahinejad, A.H. Taghvaei, S. Abdi, S. Rajabi, L. Tayebi, *Balanced enhancement of antibacterial activity and biocompatibility in chitosan-vancomycin 3D-printed scaffolds through mesoporous bioactive glass addition*, Journal of Drug Delivery Science and Technology, 105 (2025) 106637.
https://doi.org/10.1016/j.jddst.2025.106637

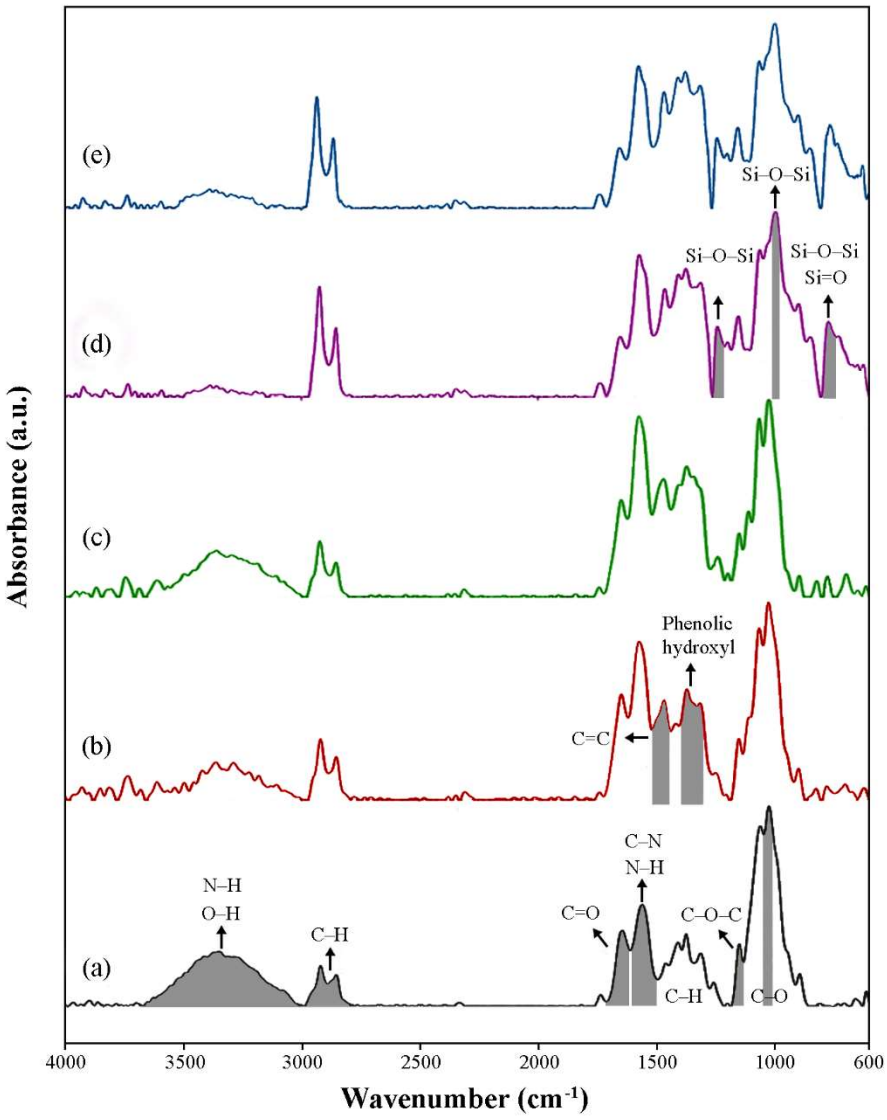

Fig. 2. FTIR spectra of Chi (a), Chi-Van (b), Chi-Van-5MBG (c), Chi-Van-10MBG (d), and Chi-Van-15MBG (e).

In the case of the samples containing MBG, the reduction in the vibrational intensity of chitosan O–H and N–H functional groups following the addition of MBG provides evidence of

This is the accepted manuscript (postprint) of the following article:
A. Parvinnasab, S. Rostami, A. Namdar, E. Salahinejad, A.H. Taghvaei, S. Abdi, S. Rajabi, L. Tayebi, *Balanced enhancement of antibacterial activity and biocompatibility in chitosan-vancomycin 3D-printed scaffolds through mesoporous bioactive glass addition*, Journal of Drug Delivery Science and Technology, 105 (2025) 106637.
https://doi.org/10.1016/j.jddst.2025.106637

chemical bonding between MBG and the polymeric matrix. The peak observed at 772 cm^{-1} can be attributed to the bending vibration of the Si–O–Si bridging group [56]. Also, the peak at 995.95 cm^{-1} is associated with the stretching vibrations of Si-O-Si bonds [57]. The appearance of the peak at 1241 cm^{-1} is assigned to the stretching vibrations of Si–O–Si bond, which can also be characterized as the longitudinal optic mode of Si-O-Si [58]. In conclusion, the FTIR analysis confirms the successful incorporation of all the components into the scaffolds, with hydrogen and electrostatic bonds among chitosan, vancomycin, and MBG.

3.2. Degradation and swelling behaviors of the scaffolds

Fig. 3 illustrates the effect of vancomycin and MBG incorporation on the degradation and swelling characteristics of the scaffolds immersed in PBS. As can be observed, over the entire immersion period, the Chi scaffold exhibits a moderate level of degradation, which can be attributed to its robust polymeric structure and the hydrolytic stability of its glycosidic bonds [59]. The addition of vancomycin leads to an increased degradation and swelling degrees, primarily due to the enhanced hydrophilicity of the scaffold [60,61], which is linked to an increase in phenolic hydroxyl groups contributed by vancomycin, as demonstrated by FTIR. Furthermore, the incorporation of MBG further accelerates both degradation and swelling rates of the scaffolds compared to the Chi and Chi-Van samples. Interestingly, this finding contrasts with most of the existing literature, which suggests that the increase of the glass content hinders the swelling and degradation of chitosan [62,63]. This discrepancy can be elucidated through considering several

This is the accepted manuscript (postprint) of the following article:
A. Parvinnasab, S. Rostami, A. Namdar, E. Salahinejad, A.H. Taghvaei, S. Abdi, S. Rajabi, L. Tayebi, *Balanced enhancement of antibacterial activity and biocompatibility in chitosan-vancomycin 3D-printed scaffolds through mesoporous bioactive glass addition*, Journal of Drug Delivery Science and Technology, 105 (2025) 106637.
https://doi.org/10.1016/j.jddst.2025.106637

observations. As shown in Fig. 1, the addition of MBG changes the filament structure by forming nano- and micropores, facilitating water access to polymer chains and enhancing water absorption within the scaffold matrix. This contribution is confirmed in the SEM micrographs of the scaffolds after immersion in PBS (Fig. 3b-c). Second, the increase in the concentration of MBG incorporation enhances the roughness of the scaffold surface (Fig. 1), enhancing the surface area, water permeability, hydrophilicity, and reactivity of the filaments. Similarly, Borges *et al*. [64] fabricated chitosan scaffolds incorporating various ceramics and found that those containing MBG exhibited greater swelling capacity, attributed to the enhanced interconnected porous structure provided by MBG. Furthermore, they indicated that the scaffolds with higher ceramic contents demonstrated superior swelling capabilities relative to the chitosan scaffolds. This influence was linked to the mesoporous structure of the glass which enables greater water retention, further validating the findings of the current study.

This is the accepted manuscript (postprint) of the following article:
A. Parvinnasab, S. Rostami, A. Namdar, E. Salahinejad, A.H. Taghvaei, S. Abdi, S. Rajabi, L. Tayebi, *Balanced enhancement of antibacterial activity and biocompatibility in chitosan-vancomycin 3D-printed scaffolds through mesoporous bioactive glass addition*, Journal of Drug Delivery Science and Technology, 105 (2025) 106637.
https://doi.org/10.1016/j.jddst.2025.106637

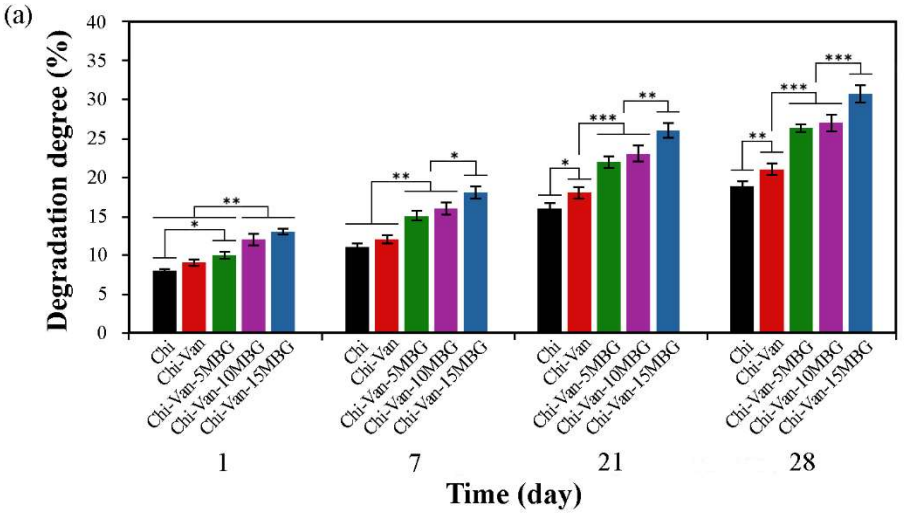

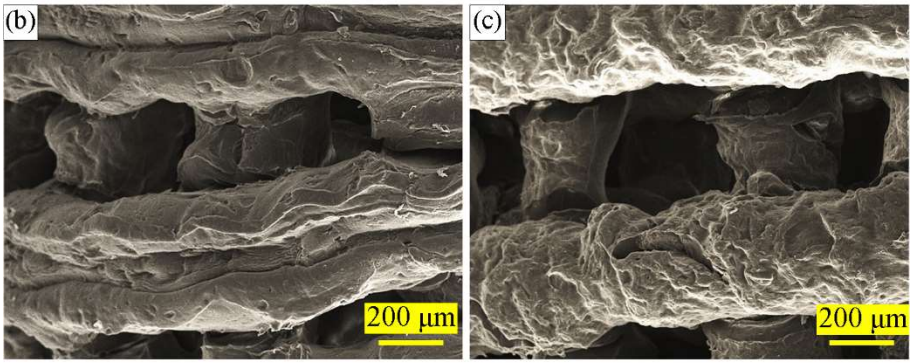

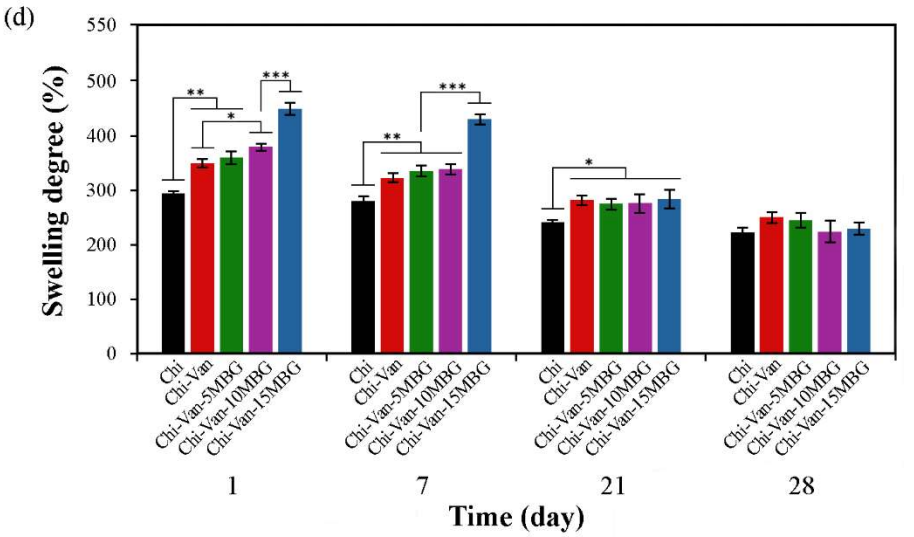

This is the accepted manuscript (postprint) of the following article:
A. Parvinnasab, S. Rostami, A. Namdar, E. Salahinejad, A.H. Taghvaei, S. Abdi, S. Rajabi, L. Tayebi, *Balanced enhancement of antibacterial activity and biocompatibility in chitosan-vancomycin 3D-printed scaffolds through mesoporous bioactive glass addition*, Journal of Drug Delivery Science and Technology, 105 (2025) 106637.
https://doi.org/10.1016/j.jddst.2025.106637

*Fig. 3. Degradation kinetics of the scaffolds in PBS (a), SEM micrograph of the Chi (b) and Chi-Van-10MBG (c) scaffolds after 7 days of immersion in PBS, and swelling degree of the scaffold in PBS (d), with *, **, and *** denoting statistically significant differences with $p < 0.05$, $p < 0.01$, and $p < 0.001$, respectively.*

Subsequent to the initial time intervals, a decline in the swelling capacity is observed across all the samples, particularly in those with the higher MBG levels. This reduction is attributed to the diminishing influence of the previously mentioned factors after one week of immersion in PBS, coupled with degradation processes that impair water retention capabilities of the scaffolds. Additionally, changes in pH due to the scaffold degradation should be considered; notably, the pH of PBS interacting with Chi-Van-10MBG shifted from 7.4 ± 0.1 to 8.2 ± 0.2 after ten days, due to the significant alkalizing effect of MBG dissolution [65], while chitosan degradation slightly reduces the local pH [66]. Such a pH increase can diminish the swelling potential of chitosan-based materials by reducing proton availability necessary for generating a positive charge on the polymeric structure [67].

According to the literature [68,69], 10-15% of carrier degradation should occur within the first day of implantation in vancomycin-loaded systems to provide a sufficient burst release for preventing biofilm formation. Also, degradation should reach 20-40% by four weeks to support the sustained release of vancomycin while preserving the scaffolds' integrity [70,71]. As shown in Fig. 3a, the degradation degree of the samples falls within these desired ranges for both burst and sustained modes, suggesting that they can act as a secure platform for local controlled vancomycin delivery. Additionally, the swelling ratio of scaffolds is critical to their performance; it should be balanced to prevent collapse while still providing benefits like improved cell attachment, nutrient

This is the accepted manuscript (postprint) of the following article:
A. Parvinnasab, S. Rostami, A. Namdar, E. Salahinejad, A.H. Taghvaei, S. Abdi, S. Rajabi, L. Tayebi, *Balanced enhancement of antibacterial activity and biocompatibility in chitosan-vancomycin 3D-printed scaffolds through mesoporous bioactive glass addition*, Journal of Drug Delivery Science and Technology, 105 (2025) 106637.
https://doi.org/10.1016/j.jddst.2025.106637

transport, water access, and effective drug release [72,73]. According to the literature, the optimal swelling ratio for systems exhibiting successful mechanical, antibacterial, and biological behaviors typically falls within the range of 200-400% [74,75]. However, using appropriate cross-linkers, chitosan matrices can withstand extreme levels of swelling as high as 900-1600% [72,73]. As indicated in Fig. 3d, the swelling ratio of the scaffolds produced in this study is in the range of 222-250% on the 28th day of PBS immersion, aligning with the well-documented optimal range.

3.3. Vancomycin release kinetics from the scaffolds

Fig. 4a represents vancomycin release profiles from the vancomycin-containing scaffolds, all impregnated with the equal amount of the drug. The first day of immersion marks the period of initial burst release, which is crucial for preventing biofilm formation. It is known that the formation of *S. aureus* biofilm can be securely prevented by vancomycin release concentrations ranging in 4-8 μg/ml within the first 24-72 h, known as the minimum inhibitory concentration (MIC) [76,77], which is satisfied by all of the drug-loaded specimen produced in this study. As stated by the American Society of Health, the therapeutic window timeframe of *S. aureus*-induced osteomyelitis treatment by vancomycin is 4-6 weeks at concentrations above the MIC [78]. Herein, all the Van-loaded systems fulfil this range.

This is the accepted manuscript (postprint) of the following article:
A. Parvinnasab, S. Rostami, A. Namdar, E. Salahinejad, A.H. Taghvaei, S. Abdi, S. Rajabi, L. Tayebi, *Balanced enhancement of antibacterial activity and biocompatibility in chitosan-vancomycin 3D-printed scaffolds through mesoporous bioactive glass addition*, Journal of Drug Delivery Science and Technology, 105 (2025) 106637.
https://doi.org/10.1016/j.jddst.2025.106637

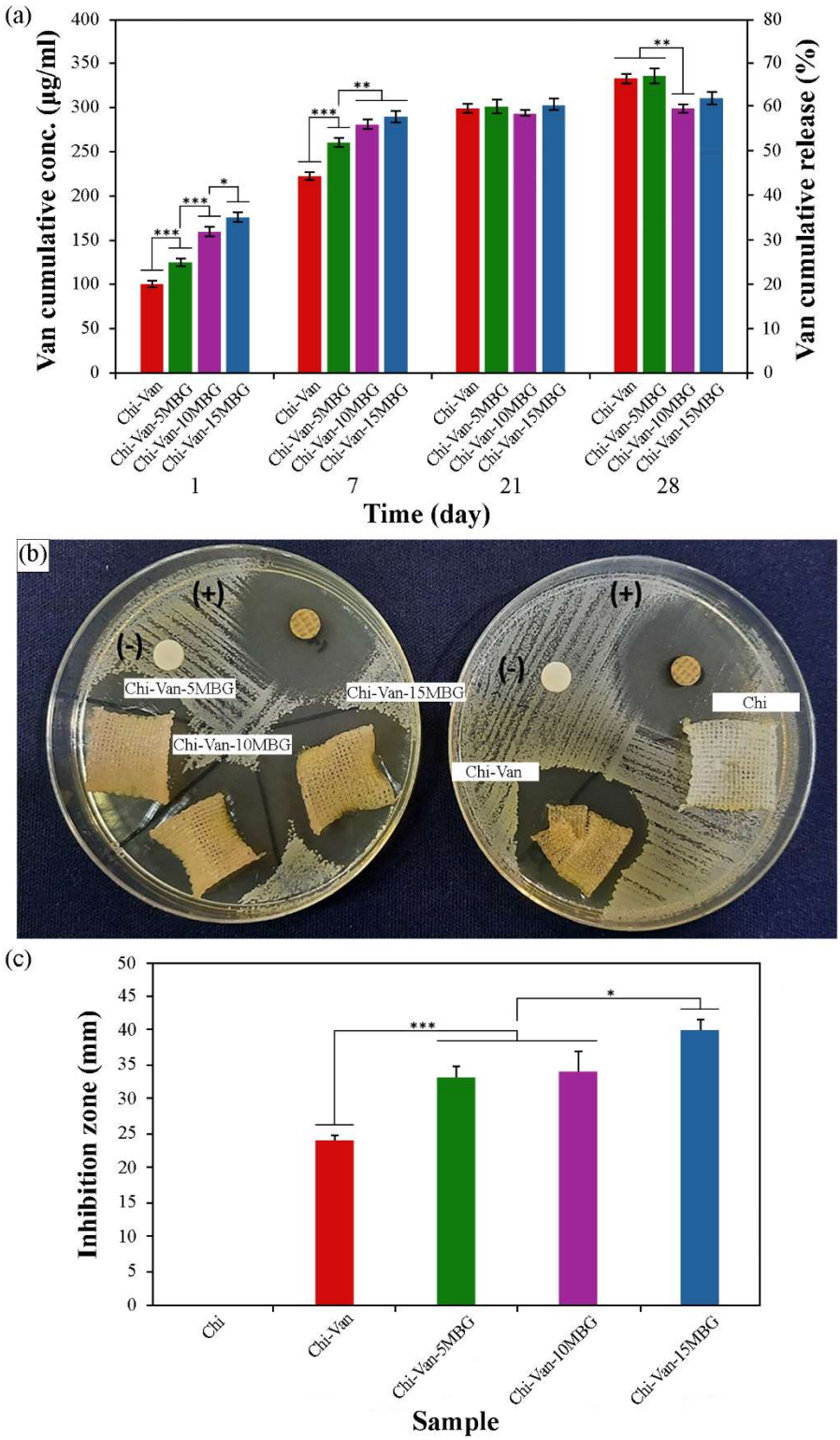

This is the accepted manuscript (postprint) of the following article:
A. Parvinnasab, S. Rostami, A. Namdar, E. Salahinejad, A.H. Taghvaei, S. Abdi, S. Rajabi, L. Tayebi, *Balanced enhancement of antibacterial activity and biocompatibility in chitosan-vancomycin 3D-printed scaffolds through mesoporous bioactive glass addition*, Journal of Drug Delivery Science and Technology, 105 (2025) 106637.
https://doi.org/10.1016/j.jddst.2025.106637

*Fig. 4. Vancomycin release profiles of the fabricated scaffolds (a), antibacterial activity testing of the prepared scaffolds along with the positive and negative controls (b), and extracted inhibition zone diameters (c), with *, **, and *** denoting statistically significant differences with $p < 0.05$, $p < 0.01$, and $p < 0.001$, respectively.*

The release concentration of vancomycin increases with the MBG content up to 7 days. However, this direct relationship diminishes by day 21 and even is reversed by day 28, resulting in cumulative release concentrations for Chi-Van-10MBG and Chi-Van-15MBG being lower than those for Chi-Van and Chi-Van-5MBG by day 28. This ambiguous behavior can be explained by considering the degradation and swelling behaviors of the different samples, along with interactions between the drug molecules and MBG. In the Chi sample, all the drug molecules are located in the chitosan matrix, while in the MBG-containing samples, some of the drug molecules are adsorbed onto the MBG nanoparticles and/or entrapped in the pores of MBG [79,80]. During the initial immersion times for these samples, the drug is primarily released from the chitosan matrix, resulting in a direct relationship between the amounts of the drug release and MBG, as degradation and swelling increase with more MBG (Fig. 3). However, over time, as the matrix is depleted from the drug, the drug molecules associated with MBG become the main source of the drug. Due to their interaction at the surface and/or within the pores of MBG, these molecules encounter a stronger barrier and are released more slowly, while the source of the drug supply from the MBG-free or low-MBG samples remains the polymer matrix. Other studies have observed similar delayed drug release behaviors whenever the drug supply source is restricted to MBG [81,82], while chitosan particularly offers fast release [83,84].

This is the accepted manuscript (postprint) of the following article:
A. Parvinnasab, S. Rostami, A. Namdar, E. Salahinejad, A.H. Taghvaei, S. Abdi, S. Rajabi, L. Tayebi, *Balanced enhancement of antibacterial activity and biocompatibility in chitosan-vancomycin 3D-printed scaffolds through mesoporous bioactive glass addition*, Journal of Drug Delivery Science and Technology, 105 (2025) 106637.
https://doi.org/10.1016/j.jddst.2025.106637

3.4. Antibacterial activity of the scaffolds

The disk diffusion assay results for the antibacterial characteristics of the scaffolds are shown in Figs. 4b and 4c. Under the tested conditions, Chi exhibited no detectable antibacterial effect against *S. aureus* bacterial strains, even though chitosan is known to have antibacterial activity against a diverse range of bacterial strains [85,86]. The antibacterial efficacy of chitosan is a complex function influenced by several factors, including the chitosan source, molecular weight, degree of deacetylation, environmental pH, and specific microbial species involved [87,88]. In contrast, Chi-Van displayed an inhibitory zone of 24.05 ± 1.22 mm. Vancomycin is a tricyclic glycopeptide antibiotic which is widely regarded as a primary therapeutic option for both the prevention and treatment of infections resulting from gram-positive bacteria like *S. aureus* [60]. It works by interfering with the proper synthesis of the bacteria cell wall.

Chi-Van-5MBG and Chi-Van-10MBG indicated 32.5 ± 1.7 and 34.0 ± 3.3 mm diameter inhibition zones, respectively, while that is 40.0 ± 1.9 mm for Chi-Van-15MBG. These results mirror the trend observed in the vancomycin release kinetics analyzed by UV spectroscopy (Fig. 4a), with Chi-Van-15MBG demonstrating the fastest drug release within the first day. As well as the influence of vancomycin release, MBG participates in the antibacterial behavior via affecting the morphology and ultrastructure of *S. aureus* bacteria due to the local elevation of pH resulting from ion exchange [89,90]. It is eventually noteworthy that the bacterial inhibition zone diameters obtained in this study meet the Clinical and Laboratory Standards Institute-approved breakpoint of 15 mm to effectively manage osteomyelitis [91].

This is the accepted manuscript (postprint) of the following article:
A. Parvinnasab, S. Rostami, A. Namdar, E. Salahinejad, A.H. Taghvaei, S. Abdi, S. Rajabi, L. Tayebi, *Balanced enhancement of antibacterial activity and biocompatibility in chitosan-vancomycin 3D-printed scaffolds through mesoporous bioactive glass addition*, Journal of Drug Delivery Science and Technology, 105 (2025) 106637.
https://doi.org/10.1016/j.jddst.2025.106637

3.5. Cell-scaffold interactions

The metabolic activity of hBMSCs in contact with the samples was assessed using the MTS assay. According to the results (Fig. 5a-b), the statistically-analyzed data revealed no significant difference between the different samples on the first day (p-value > 0.05). However, the results for the third and seventh days of cell culture demonstrate a statistically significant influence of MBG impregnation. From day 1 to day 3, there was an increase in absorbance for all the sample groups, indicating cell proliferation. This increase was particularly pronounced for the Chi-Van-10MBG group, which shows a statistically significant difference compared to the other samples, achieving 118.9 ± 3.1 % cell viability in comparison to the Chi as the control group. Also, the stimulating effect of Chi-Van-15BG is even lower than that of the control group. By day 7, the MTS absorbance increased significantly for Chi-Van-5MBG and Chi-Van-10MBG, with cell viabilities of 166.7 ± 4.5 and 191.2 ± 3.2%, respectively. In contrast, Chi-Van-15MBG decreased to 97.7 ± 4.1%. This highlights the parabolic effect of MBG on cellular response, as observed in other studies [81,92].

This is the accepted manuscript (postprint) of the following article:
A. Parvinnasab, S. Rostami, A. Namdar, E. Salahinejad, A.H. Taghvaei, S. Abdi, S. Rajabi, L. Tayebi, *Balanced enhancement of antibacterial activity and biocompatibility in chitosan-vancomycin 3D-printed scaffolds through mesoporous bioactive glass addition*, Journal of Drug Delivery Science and Technology, 105 (2025) 106637.
https://doi.org/10.1016/j.jddst.2025.106637

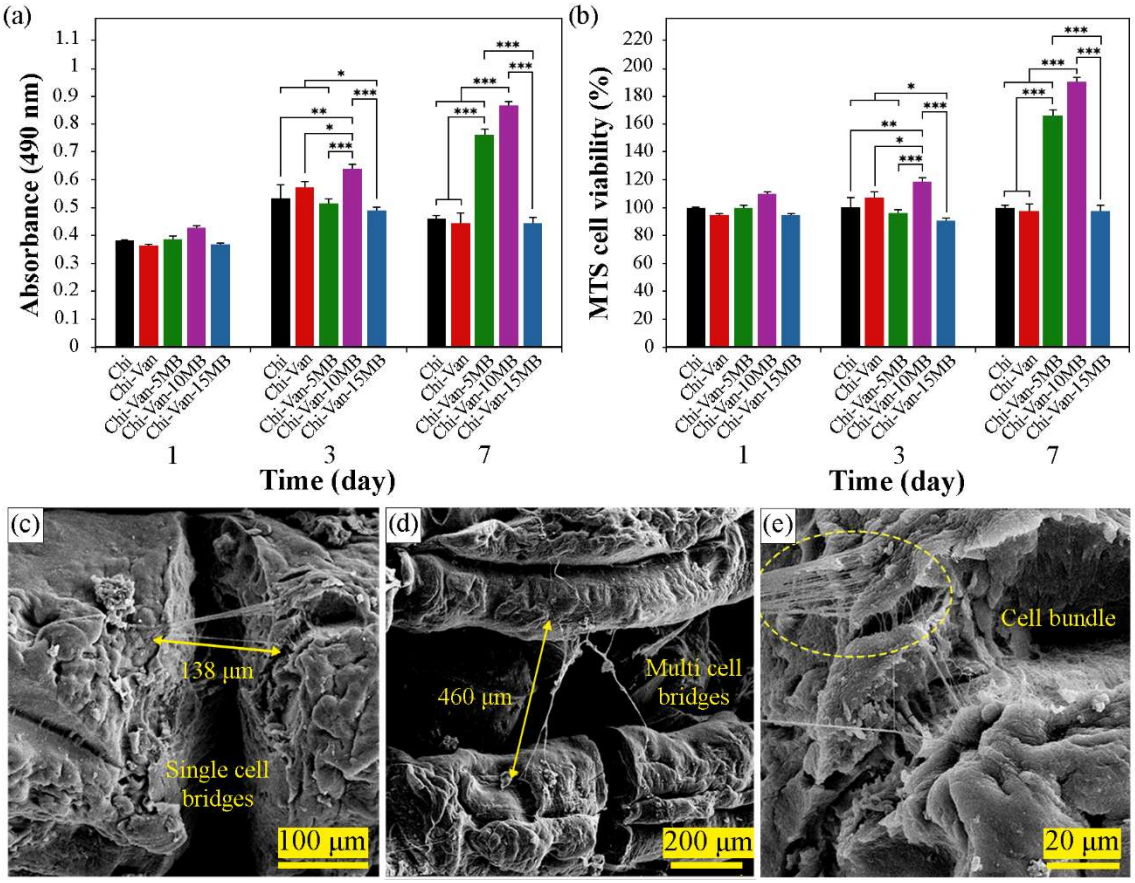

*Fig. 5. MTS assay absorbance results of the fabricated scaffolds at 490 nm (a) and corresponding cell viability results compared to the Chi sample at each time frame (b), with *, **, and *** denoting statistically significant differences with $p < 0.05$, $p < 0.01$, and $p < 0.001$, respectively. SEM images of the cell-scaffold interactions: single-cell bridging (c), multi-cell bridging (d), and cell bundles (e) on Chi-Van-10MBG.*

The cytotoxic effect of bioactive glass dissolution at high levels has been previously documented. Hench *et al*. [93] confirmed that bioactive glass ionic dissolution byproducts at high concentrations can negatively affect cell cycles. Cillardo *et al*. [94,95] also investigated bioactive glass-induced cytotoxicity in two distinct studies and declared that while low concentrations of

This is the accepted manuscript (postprint) of the following article:
A. Parvinnasab, S. Rostami, A. Namdar, E. Salahinejad, A.H. Taghvaei, S. Abdi, S. Rajabi, L. Tayebi, *Balanced enhancement of antibacterial activity and biocompatibility in chitosan-vancomycin 3D-printed scaffolds through mesoporous bioactive glass addition*, Journal of Drug Delivery Science and Technology, 105 (2025) 106637.
https://doi.org/10.1016/j.jddst.2025.106637

calcium can stimulate osteoblast cell proliferation, high concentrations cause cytotoxic effects on cells and the disruption of bone mechanosensitivity by elevated glutamate release from osteoblast cells. The localized pH change of the MTS solution at high concentrations of MBG, as well as the higher vancomycin release observed in this sample are other factors to consider when explaining the lower cell viability in the medium in contact with Chi-Van-15MBG.

To evaluate the significance of the obtained results, a comparison with published papers in this area was undertaken. In a study done by Naeimi *et al.* [96] concerning the antibacterial efficacy and cytocompatibility of vancomycin-loaded chitosan/polyvinyl alcohol (PVA) hydrogels, a zone of inhibition (ZOI) measured 19 ± 3 mm against *S. aureus* resulted in 6% reduction in a fibroblast cell viability compared to the unloaded chitosan/PVA by a two-day duration. In another work, Xu *et al.* [97] developed vancomycin-loaded N-trimethyl chitosan nanoparticles via the ionic gelation method, resulting in an inadequate ZOI of less than 6, but a notable cell viability of 168%. On the contrary, the optimal sample in the current study revealed a ZOI of 34.0 ± 3.3 mm, while maintaining consistent cell viability as high as 110.5 ± 1.8, 118.9 ± 3.1, and 191.2 ± 3.2 %, by 1, 3, and 7 days, respectively, achieved without compromising the antibacterial efficacy and cytocompatibility observed in similar studies. This significant enhancement in both antibacterial performance and cytocompatibility is due to the scaffolds' design, particularly the dual effects of MBG up to a threshold loaded value.

Figs. 5c-e illustrate micrographs of cells cultured on Chi-Van-10MBG, identified as the optimal formulation for MTS cell cytocompatibility. Notably, the cells establish connections between different points within the scaffold, forming bridges rather than merely spreading across

This is the accepted manuscript (postprint) of the following article:
A. Parvinnasab, S. Rostami, A. Namdar, E. Salahinejad, A.H. Taghvaei, S. Abdi, S. Rajabi, L. Tayebi, *Balanced enhancement of antibacterial activity and biocompatibility in chitosan-vancomycin 3D-printed scaffolds through mesoporous bioactive glass addition*, Journal of Drug Delivery Science and Technology, 105 (2025) 106637.
https://doi.org/10.1016/j.jddst.2025.106637

the surface. The observation of single-cell bridging within a 138-µm gap (Fig. 5c) and multi-cell bridging over a distance of 460 µm (Fig. 5d) provides strong evidence of effective cell-substrate interactions. Interestingly, the latter distance exceeds the highest reported value of 400 µm for MSCs [98]. Moreover, the formation of cell bundles, as shown in Fig. 5e, is another observed phenomenon, resulting from cell migration toward adhesive points. These morphological findings accentuate that although the interaction of hMSCs with the fabricated scaffold may not overtly demonstrate extensive spanning across the scaffolds, the structural properties of the 3D-printed scaffolds facilitate cell interactions through pulling forces. These forces lead to the formation of bridges between the scaffold points, along with robust cell adherence. The observed bridging attachments suggest that Chi-Van-10MBG can enhance cell proliferation, migration, and interactions with extracellular matrix (ECM), maintain tissue integrity, and facilitate bone tissue regeneration *in vivo* [99].

4. Conclusion

In this study, 3D-printed chitosan/mesoporous bioactive glass/vancomycin scaffolds were developed and their potential for osteomyelitis treatment was evaluated *in vitro*. Scanning electron microscopy revealed that the scaffolds, with an interconnected porous structure and proper pore size, effectively promote cell viability, proliferation, and attachment. The fabricated scaffolds exhibited an initial burst vancomycin release followed by sustained release over 4 weeks, indicating its ability to provide prolonged infection control. The scaffolds demonstrated significant

This is the accepted manuscript (postprint) of the following article:
A. Parvinnasab, S. Rostami, A. Namdar, E. Salahinejad, A.H. Taghvaei, S. Abdi, S. Rajabi, L. Tayebi, *Balanced enhancement of antibacterial activity and biocompatibility in chitosan-vancomycin 3D-printed scaffolds through mesoporous bioactive glass addition*, Journal of Drug Delivery Science and Technology, 105 (2025) 106637.
https://doi.org/10.1016/j.jddst.2025.106637

antibacterial activity against *S. aureus*, the primary pathogen in osteomyelitis, while maintaining high cytocompatibility with hBMSCs. Notably, the optimal sample in this study, Chi-Van-10MBG, could offer a promising therapeutic strategy for osteomyelitis by achieving a balanced enhancement of antibacterial activity and cell biocompatibility. The bridging attachments of hBMSCs to this sample help compensate for the limitations of chitosan-based scaffolds in interacting with and attaching to the cells. However, future work should focus on *in vivo* validation of the scaffold efficacy and safety in relevant animal osteomyelitis models. Studies evaluating bone defect healing, infection resolution, scaffold degradation and immunogenicity over extended time points could provide essential data to support potential clinical translation.

Acknowledgment

L.T. acknowledges the support from National Institutes of Health under award numbers R56 DE029191 and 1R21EY035480-01.

References

[1] R.A.A. Muzzarelli, M. Mattioli-Belmonte, C. Tietz, R. Biagini, G. Ferioli, M.A. Brunelli, M. Fini, R. Giardino, P. Ilari, G. Biagini, Stimulatory effect on bone formation exerted by a modified chitosan, Biomaterials 15 (1994) 1075–1081. https://doi.org/10.1016/0142-9612(94)90093-0.

[2] Y.J. Seol, J.Y. Lee, Y.J. Park, Y.M. Lee, Y. -Ku, I.C. Rhyu, S.J. Lee, S.B. Han, C.P. Chung, Chitosan sponges as tissue engineering scaffolds for bone formation, Biotechnol. Lett. 26 (2004) 1037–1041. https://doi.org/10.1023/B:BILE.0000032962.79531.FD/METRICS.

[3] X. Zhao, P. Li, J. Zhu, Y. Xia, J. Ma, X. Pu, Y. Wang, F. Leng, Y. Wang, S. Yang, F. Ran, D. Tang,

This is the accepted manuscript (postprint) of the following article:
A. Parvinnasab, S. Rostami, A. Namdar, E. Salahinejad, A.H. Taghvaei, S. Abdi, S. Rajabi, L. Tayebi, *Balanced enhancement of antibacterial activity and biocompatibility in chitosan-vancomycin 3D-printed scaffolds through mesoporous bioactive glass addition*, Journal of Drug Delivery Science and Technology, 105 (2025) 106637.
https://doi.org/10.1016/j.jddst.2025.106637

W. Zhang, Polygonatum polysaccharide modified montmorillonite/chitosan/glycerophosphate composite hydrogel for bone tissue engineering, Int. J. Polym. Mater. Polym. Biomater. 71 (2022) 1176–1187. https://doi.org/10.1080/00914037.2021.1960336.

[4] A. Di Martino, M. Sittinger, M. V. Risbud, Chitosan: a versatile biopolymer for orthopaedic tissue-engineering, Biomaterials 26 (2005) 5983–5990. https://doi.org/10.1016/J.BIOMATERIALS.2005.03.016.

[5] E. Szymańska, K. Winnicka, Stability of Chitosan—A Challenge for Pharmaceutical and Biomedical Applications, Mar. Drugs 13 (2015) 1819. https://doi.org/10.3390/MD13041819.

[6] R. Song, M. Murphy, C. Li, K. Ting, C. Soo, Z. Zheng, Current development of biodegradable polymeric materials for biomedical applications, Drug Des. Devel. Ther. 12 (2018) 3117. https://doi.org/10.2147/DDDT.S165440.

[7] S. Mekahlia, B. Bouzid, Chitosan-Copper (II) complex as antibacterial agent: synthesis, characterization and coordinating bond- activity correlation study, Phys. Procedia 2 (2009) 1045–1053. https://doi.org/10.1016/J.PHPRO.2009.11.061.

[8] S. Shahroudi, A. Parvinnasab, E. Salahinejad, S. Abdi, S. Rajabi, L. Tayebi, Efficacy of 3D-printed chitosan-cerium oxide dressings coated with vancomycin-loaded alginate for chronic wounds management, Carbohydr. Polym. 349 (2025) 123036. https://doi.org/10.1016/J.CARBPOL.2024.123036.

[9] Z. Yang, J. Liu, J. Gao, S. Chen, G. Huang, Chitosan coated vancomycin hydrochloride liposomes: Characterizations and evaluation, Int. J. Pharm. 495 (2015) 508–515. https://doi.org/10.1016/J.IJPHARM.2015.08.085.

[10] E. Cevher, Z. Orhan, L. Mülazimoğlu, D. Şensoy, M. Alper, A. Yildiz, Y. Özsoy, Characterization of biodegradable chitosan microspheres containing vancomycin and treatment of experimental osteomyelitis caused by methicillin-resistant Staphylococcus aureus with prepared microspheres, Int. J. Pharm. 317 (2006) 127–135. https://doi.org/10.1016/J.IJPHARM.2006.03.014.

[11] C.A. García-González, J. Barros, A. Rey-Rico, P. Redondo, J.L. Gómez-Amoza, A. Concheiro, C. Alvarez-Lorenzo, F.J. Monteiro, Antimicrobial Properties and Osteogenicity of Vancomycin-Loaded Synthetic Scaffolds Obtained by Supercritical Foaming, ACS Appl. Mater. Interfaces 10 (2018) 3349–3360. https://doi.org/10.1021/ACSAMI.7B17375/SUPPL_FILE/AM7B17375_SI_001.PDF.

[12] L.J.R. Foster, K. Thomson, H. Marçal, J. Butt, S.L. Watson, D. Wakefield, Chitosan-vancomysin composite biomaterial as a laser activated surgical adhesive with regional antimicrobial activity, Biomacromolecules 11 (2010) 3563–3570. https://doi.org/10.1021/BM101028G/ASSET/IMAGES/MEDIUM/BM-2010-01028G_0002.GIF.

[13] S.P. Chakraborty, S.K. Sahu, P. Pramanik, S. Roy, In vitro antimicrobial activity of nanoconjugated vancomycin against drug resistant Staphylococcus aureus, Int. J. Pharm. 436 (2012) 659–676. https://doi.org/10.1016/J.IJPHARM.2012.07.033.

[14] C. López-Iglesias, J. Barros, I. Ardao, F.J. Monteiro, C. Alvarez-Lorenzo, J.L. Gómez-Amoza, C.A. García-González, Vancomycin-loaded chitosan aerogel particles for chronic wound applications, Carbohydr. Polym. 204 (2019) 223–231. https://doi.org/10.1016/J.CARBPOL.2018.10.012.

This is the accepted manuscript (postprint) of the following article:
A. Parvinnasab, S. Rostami, A. Namdar, E. Salahinejad, A.H. Taghvaei, S. Abdi, S. Rajabi, L. Tayebi, *Balanced enhancement of antibacterial activity and biocompatibility in chitosan-vancomycin 3D-printed scaffolds through mesoporous bioactive glass addition*, Journal of Drug Delivery Science and Technology, 105 (2025) 106637.
https://doi.org/10.1016/j.jddst.2025.106637

[15] C.W. James, C. Gurk-Turner, Recommendations for Monitoring Serum Vancomycin Concentrations, Baylor Univ. Med. Cent. Proc. 14 (2001) 189–190. https://doi.org/10.1080/08998280.2001.11927763.

[16] L.K. Hidayat, D.I. Hsu, R. Quist, K.A. Shriner, A. Wong-Beringer, High-Dose Vancomycin Therapy for Methicillin-Resistant Staphylococcus aureus Infections: Efficacy and Toxicity, Arch. Intern. Med. 166 (2006) 2138–2144. https://doi.org/10.1001/ARCHINTE.166.19.2138.

[17] D.L. Lameire, J. Soeder, H. Abdel Khalik, E. Pinsker, N. Atri, A. Khoshbin, L. Radomski, A. Atrey, Local vancomycin administration in Orthopaedic Surgery - A systematic review of comparative studies, J. Orthop. 55 (2024) 44–58. https://doi.org/10.1016/J.JOR.2024.03.040.

[18] C.T. Chen, K.J. Ng, Y. Lin, M.C. Kao, Red man syndrome following the use of vancomycin-loaded bone cement in the primary total knee replacement: A case report, Medicine (Baltimore). 97 (2018). https://doi.org/10.1097/MD.0000000000013371.

[19] T.J. Martel, R.T. Jamil, K.C. King, Vancomycin Flushing Syndrome, Am. Nurse J. 18 (2023) 26–26. https://doi.org/10.51256/anj102326.

[20] J. Braun, S. Eckes, P.M. Rommens, K. Schmitz, D. Nickel, U. Ritz, Toxic Effect of Vancomycin on Viability and Functionality of Different Cells Involved in Tissue Regeneration, Antibiotics 9 (2020). https://doi.org/10.3390/ANTIBIOTICS9050238.

[21] J.X. Liu, D. Bravo, J. Buza, T. Kirsch, O. Kennedy, A. Rokito, J.D. Zuckerman, M.S. Virk, Topical vancomycin and its effect on survival and migration of osteoblasts, fibroblasts, and myoblasts: An in vitro study, J. Orthop. 15 (2018) 53–58. https://doi.org/10.1016/J.JOR.2018.01.032.

[22] A. Namdar, E. Salahinejad, Advances in ion-doping of Ca-Mg silicate bioceramics for bone tissue engineering, Coord. Chem. Rev. 478 (2023) 215001. https://doi.org/10.1016/J.CCR.2022.215001.

[23] R. Keihan, A.R. Ghorbani, E. Salahinejad, E. Sharifi, L. Tayebi, Biomineralization, strength and cytocompatibility improvement of bredigite scaffolds through doping/coating, Ceram. Int. 46 (2020) 21056–21063. https://doi.org/10.1016/J.CERAMINT.2020.05.178.

[24] R. Aqib, S. Kiani, S. Bano, A. Wadood, M.A. Ur Rehman, Ag–Sr doped mesoporous bioactive glass nanoparticles loaded chitosan/gelatin coating for orthopedic implants, Int. J. Appl. Ceram. Technol. 18 (2021) 544–562. https://doi.org/10.1111/IJAC.13702.

[25] F. Boschetto, H.N. Doan, P.P. Vo, M. Zanocco, W. Zhu, W. Sakai, T. Adachi, E. Ohgitani, N. Tsutsumi, O. Mazda, K. Kinashi, E. Marin, G. Pezzotti, Antibacterial and Osteoconductive Effects of Chitosan/Polyethylene Oxide (PEO)/Bioactive Glass Nanofibers for Orthopedic Applications, Appl. Sci. 2020, Vol. 10, Page 2360 10 (2020) 2360. https://doi.org/10.3390/APP10072360.

[26] F. Pishbin, V. Mouriño, J.B. Gilchrist, D.W. McComb, S. Kreppel, V. Salih, M.P. Ryan, A.R. Boccaccini, Single-step electrochemical deposition of antimicrobial orthopaedic coatings based on a bioactive glass/chitosan/nano-silver composite system, Acta Biomater. 9 (2013) 7469–7479. https://doi.org/10.1016/J.ACTBIO.2013.03.006.

[27] R. Zeeshan, Z. Mutahir, H. Iqbal, M. Ali, F. Iqbal, K. Ijaz, F. Sharif, A.T. Shah, A.A. Chaudhry, M. Yar, S. Luan, A.F. Khan, Ihtesham-ur-Rehman, Hydroxypropylmethyl cellulose (HPMC) crosslinked chitosan (CH) based scaffolds containing bioactive glass (BG) and zinc oxide (ZnO) for alveolar bone repair, Carbohydr. Polym. 193 (2018) 9–18.

This is the accepted manuscript (postprint) of the following article:
A. Parvinnasab, S. Rostami, A. Namdar, E. Salahinejad, A.H. Taghvaei, S. Abdi, S. Rajabi, L. Tayebi, *Balanced enhancement of antibacterial activity and biocompatibility in chitosan-vancomycin 3D-printed scaffolds through mesoporous bioactive glass addition*, Journal of Drug Delivery Science and Technology, 105 (2025) 106637.
https://doi.org/10.1016/j.jddst.2025.106637

https://doi.org/10.1016/J.CARBPOL.2018.03.046.

[28] A.M. El-Kady, N.A. Kamel, M.M. Elnashar, M.M. Farag, Production of bioactive glass/chitosan scaffolds by freeze-gelation for optimized vancomycin delivery: Effectiveness of glass presence on controlling the drug release kinetics, J. Drug Deliv. Sci. Technol. 66 (2021) 102779. https://doi.org/10.1016/J.JDDST.2021.102779.

[29] X. Zhang, D. Zeng, N. Li, J. Wen, X. Jiang, C. Liu, Y. Li, Functionalized mesoporous bioactive glass scaffolds for enhanced bone tissue regeneration, Sci. Reports 2016 61 6 (2016) 1–12. https://doi.org/10.1038/srep19361.

[30] M. Salètes, M. Vartin, C. Mocquot, C. Chevalier, B. Grosgogeat, P. Colon, N. Attik, Mesoporous Bioactive Glasses Cytocompatibility Assessment: A Review of In Vitro Studies, Biomimetics 2021, Vol. 6, Page 9 6 (2021) 9. https://doi.org/10.3390/BIOMIMETICS6010009.

[31] M. Vallet-Regi, A.J. Salinas, Mesoporous bioactive glasses for regenerative medicine, Mater. Today Bio 11 (2021) 100121. https://doi.org/10.1016/J.MTBIO.2021.100121.

[32] F. Westhauser, S. Decker, Q. Nawaz, F. Rehder, S. Wilkesmann, A. Moghaddam, E. Kunisch, A.R. Boccaccini, Impact of Zinc- or Copper-Doped Mesoporous Bioactive Glass Nanoparticles on the Osteogenic Differentiation and Matrix Formation of Mesenchymal Stromal Cells, Mater. 2021, Vol. 14, Page 1864 14 (2021) 1864. https://doi.org/10.3390/MA14081864.

[33] N. Gómez-Cerezo, L. Casarrubios, I. Morales, M.J. Feito, M. Vallet-Regí, D. Arcos, M.T. Portolés, Effects of a mesoporous bioactive glass on osteoblasts, osteoclasts and macrophages, J. Colloid Interface Sci. 528 (2018) 309–320. https://doi.org/10.1016/J.JCIS.2018.05.099.

[34] M. Alcaide, P. Portolés, A. López-Noriega, D. Arcos, M. Vallet-Regí, M.T. Portolés, Interaction of an ordered mesoporous bioactive glass with osteoblasts, fibroblasts and lymphocytes, demonstrating its biocompatibility as a potential bone graft material, Acta Biomater. 6 (2010) 892–899. https://doi.org/10.1016/J.ACTBIO.2009.09.008.

[35] C. Migneco, E. Fiume, E. Verné, F. Baino, A Guided Walk through the World of Mesoporous Bioactive Glasses (MBGs): Fundamentals, Processing, and Applications, Nanomater. 2020, Vol. 10, Page 2571 10 (2020) 2571. https://doi.org/10.3390/NANO10122571.

[36] A. Munir, D. Marovic, L.P. Nogueira, R. Simm, A.O. Naemi, S.M. Landrø, M. Helgerud, K. Zheng, M. Par, T.T. Tauböck, T. Attin, Z. Tarle, A.R. Boccaccini, H.J. Haugen, Using Copper-Doped Mesoporous Bioactive Glass Nanospheres to Impart Anti-Bacterial Properties to Dental Composites, Pharm. 2022, Vol. 14, Page 2241 14 (2022) 2241. https://doi.org/10.3390/PHARMACEUTICS14102241.

[37] K. Zheng, P. Balasubramanian, T.E. Paterson, R. Stein, S. MacNeil, S. Fiorilli, C. Vitale-Brovarone, J. Shepherd, A.R. Boccaccini, Ag modified mesoporous bioactive glass nanoparticles for enhanced antibacterial activity in 3D infected skin model, Mater. Sci. Eng. C 103 (2019) 109764. https://doi.org/10.1016/J.MSEC.2019.109764.

[38] M. Hosseini, N. Hassani Besheli, D. Deng, C. Lievens, Y. Zuo, S.C.G. Leeuwenburgh, F. Yang, Facile post modification synthesis of copper-doped mesoporous bioactive glass with high antibacterial performance to fight bone infection, Biomater. Adv. 144 (2023) 213198. https://doi.org/10.1016/J.BIOADV.2022.213198.

This is the accepted manuscript (postprint) of the following article:
A. Parvinnasab, S. Rostami, A. Namdar, E. Salahinejad, A.H. Taghvaei, S. Abdi, S. Rajabi, L. Tayebi, *Balanced enhancement of antibacterial activity and biocompatibility in chitosan-vancomycin 3D-printed scaffolds through mesoporous bioactive glass addition*, Journal of Drug Delivery Science and Technology, 105 (2025) 106637.
https://doi.org/10.1016/j.jddst.2025.106637

[39] S. Kaya, M. Cresswell, A.R. Boccaccini, Mesoporous silica-based bioactive glasses for antibiotic-free antibacterial applications, Mater. Sci. Eng. C 83 (2018) 99–107. https://doi.org/10.1016/J.MSEC.2017.11.003.

[40] P. Nooeaid, W. Li, J.A. Roether, V. Mouriño, O.-M. Goudouri, D.W. Schubert, A.R. Boccaccini, Development of bioactive glass based scaffolds for controlled antibiotic release in bone tissue engineering via biodegradable polymer layered coating, Biointerphases 9 (2014) 041001. https://doi.org/10.1116/1.4897217/133796.

[41] P. Zhou, Y. Xia, J. Wang, C. Liang, L. Yu, W. Tang, S. Gu, S. Xu, Antibacterial properties and bioactivity of HACC- and HACC–Zein-modified mesoporous bioactive glass scaffolds, J. Mater. Chem. B 1 (2013) 685–692. https://doi.org/10.1039/C2TB00102K.

[42] S. Khanmohammadi, H. Aghajani, Electrophoretic deposition of ternary chitosan/mesoporous bioglass/hydroxyapatite composite coatings for drug delivery application, Bull. Mater. Sci. 47 (2024) 1–10. https://doi.org/10.1007/S12034-023-03125-9/METRICS.

[43] S. Khanmohammadi, H. Aghajani, M. Farrokhi-Rad, Vancomycin loaded-mesoporous bioglass/hydroxyapatite/chitosan coatings by electrophoretic deposition, Ceram. Int. 48 (2022) 20176–20186. https://doi.org/10.1016/J.CERAMINT.2022.03.296.

[44] H.A. Doty, M.R. Leedy, H.S. Courtney, W.O. Haggard, J.D. Bumgardner, Composite chitosan and calcium sulfate scaffold for dual delivery of vancomycin and recombinant human bone morphogenetic protein-2, J. Mater. Sci. Mater. Med. 25 (2014) 1449–1459. https://doi.org/10.1007/S10856-014-5167-7.

[45] I. López-González, A.B. Hernández-Heredia, M.I. Rodríguez-López, D. Auñón-Calles, M. Boudifa, J.A. Gabaldón, L. Meseguer-Olmo, Evaluation of the In Vitro Antimicrobial Efficacy against Staphylococcus aureus and epidermidis of a Novel 3D-Printed Degradable Drug Delivery System Based on Polycaprolactone/Chitosan/Vancomycin-Preclinical Study, Pharmaceutics 15 (2023). https://doi.org/10.3390/PHARMACEUTICS15061763.

[46] S.Y. Hann, H. Cui, T. Esworthy, X. Zhou, S. jun Lee, M.W. Plesniak, L.G. Zhang, Dual 3D printing for vascularized bone tissue regeneration, Acta Biomater. 123 (2021) 263–274. https://doi.org/10.1016/J.ACTBIO.2021.01.012.

[47] S. V. Murphy, A. Atala, 3D bioprinting of tissues and organs, Nat. Biotechnol. 2014 328 32 (2014) 773–785. https://doi.org/10.1038/nbt.2958.

[48] E.B. Toloue, M. Mohammadalipour, S. Mukherjee, S. Karbasi, Ultra-thin electrospun nanocomposite scaffold of poly (3-hydroxybutyrate)-chitosan/magnetic mesoporous bioactive glasses for bone tissue engineering applications, Int. J. Biol. Macromol. 254 (2024) 127860. https://doi.org/10.1016/J.IJBIOMAC.2023.127860.

[49] A.C. Vale, P. Pereira, A.M. Barbosa, E. Torrado, J.F. Mano, N.M. Alves, Antibacterial free-standing polysaccharide composite films inspired by the sea, Int. J. Biol. Macromol. 133 (2019) 933–944. https://doi.org/10.1016/J.IJBIOMAC.2019.04.102.

[50] T. Tallei, Structural Characteristics of Chitin and Chitosan Isolated from the Biomass of Cultivated Rotifer, Brachionus rotundiformis., (2014).

[51] A. Parvinnasab, S. Shahroudi, E. Salahinejad, A.H. Taghvaei, S.A. Sharifi Fard, E. Sharifi,

This is the accepted manuscript (postprint) of the following article:
A. Parvinnasab, S. Rostami, A. Namdar, E. Salahinejad, A.H. Taghvaei, S. Abdi, S. Rajabi, L. Tayebi, *Balanced enhancement of antibacterial activity and biocompatibility in chitosan-vancomycin 3D-printed scaffolds through mesoporous bioactive glass addition*, Journal of Drug Delivery Science and Technology, 105 (2025) 106637.
https://doi.org/10.1016/j.jddst.2025.106637

Antibacterial nanofibrous wound dressing mats made from blended chitosan-copper complexes and polyvinyl alcohol (PVA) using electrospinning, Carbohydr. Polym. Technol. Appl. 8 (2024) 100564. https://doi.org/10.1016/J.CARPTA.2024.100564.

[52] C. Paluszkiewicz, E. Stodolak, M. Hasik, M. Blazewicz, FT-IR study of montmorillonite–chitosan nanocomposite materials, Spectrochim. Acta Part A Mol. Biomol. Spectrosc. 79 (2011) 784–788. https://doi.org/10.1016/J.SAA.2010.08.053.

[53] A. Kaur, D. Goyal, R. Kumar, Surfactant mediated interaction of vancomycin with silver nanoparticles, Appl. Surf. Sci. 449 (2018) 23–30. https://doi.org/10.1016/J.APSUSC.2017.12.066.

[54] H.B. Mohamed, S.M. El-Shanawany, M.A. Hamad, M. Elsabahy, Niosomes: A Strategy toward Prevention of Clinically Significant Drug Incompatibilities, Sci. Reports 2017 71 7 (2017) 1–14. https://doi.org/10.1038/s41598-017-06955-w.

[55] Q. Yao, P. Nooeaid, J.A. Roether, Y. Dong, Q. Zhang, A.R. Boccaccini, Bioglass®-based scaffolds incorporating polycaprolactone and chitosan coatings for controlled vancomycin delivery, Ceram. Int. 39 (2013) 7517–7522. https://doi.org/10.1016/J.CERAMINT.2013.03.002.

[56] K. Przykaza, M. Jurak, G. Kalisz, R. Mroczka, A.E. Wiącek, Characteristics of Hybrid Bioglass-Chitosan Coatings on the Plasma Activated PEEK Polymer, Mol. 2023, Vol. 28, Page 1729 28 (2023) 1729. https://doi.org/10.3390/MOLECULES28041729.

[57] R. Ellerbrock, M. Stein, J. Schaller, Comparing amorphous silica, short-range-ordered silicates and silicic acid species by FTIR, Sci. Reports 2022 121 12 (2022) 1–8. https://doi.org/10.1038/s41598-022-15882-4.

[58] D. Skácelová, P. Sládek, P. Stahel, L. Pawera, M. Haničinec, J. Meichsner, M. Černák, Properties of atmospheric pressure plasma oxidized layers on silicon wafers, Open Chem. 13 (2015) 376–381. https://doi.org/10.1515/CHEM-2015-0047/MACHINEREADABLECITATION/RIS.

[59] C.P. Jiménez-Gómez, J.A. Cecilia, Chitosan: A Natural Biopolymer with a Wide and Varied Range of Applications, Mol. 2020, Vol. 25, Page 3981 25 (2020) 3981. https://doi.org/10.3390/MOLECULES25173981.

[60] M. Darestani-Farahani, E. Vasheghani-Farahani, H. Mobedi, F. Ganji, The effect of solvent composition on vancomycin hydrochloride and free base vancomycin release from in situ forming implants, Polym. Adv. Technol. 27 (2016) 1653–1663. https://doi.org/10.1002/PAT.3845.

[61] X. Gao, Z. Xu, S. Li, L. Cheng, D. Xu, L. Li, L. Chen, Y. Xu, Z. Liu, Y. Liu, J. Sun, Chitosan-vancomycin hydrogel incorporated bone repair scaffold based on staggered orthogonal structure: a viable dually controlled drug delivery system, RSC Adv. 13 (2023) 3759–3765. https://doi.org/10.1039/D2RA07828G.

[62] M. Peter, N.S. Binulal, S. V. Nair, N. Selvamurugan, H. Tamura, R. Jayakumar, Novel biodegradable chitosan–gelatin/nano-bioactive glass ceramic composite scaffolds for alveolar bone tissue engineering, Chem. Eng. J. 158 (2010) 353–361. https://doi.org/10.1016/J.CEJ.2010.02.003.

[63] M. Peter, N.S. Binulal, S. Soumya, S. V. Nair, T. Furuike, H. Tamura, R. Jayakumar, Nanocomposite scaffolds of bioactive glass ceramic nanoparticles disseminated chitosan matrix for tissue engineering applications, Carbohydr. Polym. 79 (2010) 284–289. https://doi.org/10.1016/J.CARBPOL.2009.08.001.

This is the accepted manuscript (postprint) of the following article:
A. Parvinnasab, S. Rostami, A. Namdar, E. Salahinejad, A.H. Taghvaei, S. Abdi, S. Rajabi, L. Tayebi, *Balanced enhancement of antibacterial activity and biocompatibility in chitosan-vancomycin 3D-printed scaffolds through mesoporous bioactive glass addition*, Journal of Drug Delivery Science and Technology, 105 (2025) 106637.
https://doi.org/10.1016/j.jddst.2025.106637

[64] A.S. Pádua, L. Figueiredo, J.C. Silva, J.P. Borges, Chitosan scaffolds with mesoporous hydroxyapatite and mesoporous bioactive glass, Prog. Biomater. 12 (2023) 137–153. https://doi.org/10.1007/S40204-023-00217-X/FIGURES/12.

[65] L. Drago, M. Toscano, M. Bottagisio, Recent Evidence on Bioactive Glass Antimicrobial and Antibiofilm Activity: A Mini-Review, Materials (Basel). 11 (2018). https://doi.org/10.3390/MA11020326.

[66] N. Desai, D. Rana, S. Salave, R. Gupta, P. Patel, B. Karunakaran, A. Sharma, J. Giri, D. Benival, N. Kommineni, Chitosan: A Potential Biopolymer in Drug Delivery and Biomedical Applications, Pharm. 2023, Vol. 15, Page 1313 15 (2023) 1313. https://doi.org/10.3390/PHARMACEUTICS15041313.

[67] M.M. Abd El-Hady, S. El-Sayed Saeed, Antibacterial Properties and pH Sensitive Swelling of Insitu Formed Silver-Curcumin Nanocomposite Based Chitosan Hydrogel, Polymers (Basel). 12 (2020) 1–14. https://doi.org/10.3390/POLYM12112451.

[68] R. Ravarian, M. Craft, F. Dehghani, Enhancing the biological activity of chitosan and controlling the degradation by nanoscale interaction with bioglass, J. Biomed. Mater. Res. A 103 (2015) 2898–2908. https://doi.org/10.1002/JBM.A.35423.

[69] N. Akhlaghi, G. Najafpour-Darzi, Thermosensitive injectable dual drug-loaded chitosan-based hybrid hydrogel for treatment of orthopedic implant infections, Carbohydr. Polym. 320 (2023). https://doi.org/10.1016/J.CARBPOL.2023.121138.

[70] B. Kaczmarek, K. Nadolna, A. Owczarek, O. Mazur, A. Sionkowska, K. Łukowicz, J. Vishnu, G. Manivasagam, A.M. Osyczka, Properties of scaffolds based on chitosan and collagen with bioglass 45S5, IET Nanobiotechnology 14 (2020) 830–832. https://doi.org/10.1049/IET-NBT.2020.0045.

[71] E. Alsberg, H.J. Kong, Y. Hirano, M.K. Smith, A. Albeiruti, D.J. Mooney, Regulating Bone Formation via Controlled Scaffold Degradation, Http://Dx.Doi.Org/10.1177/154405910308201111 82 (2003) 903–908. https://doi.org/10.1177/154405910308201111.

[72] M. Biernat, A. Woźniak, M. Chraniuk, M. Panasiuk, P. Tymowicz-Grzyb, J. Pagacz, A. Antosik, L. Ciołek, B. Gromadzka, Z. Jaegermann, Effect of Selected Crosslinking and Stabilization Methods on the Properties of Porous Chitosan Composites Dedicated for Medical Applications, Polym. 2023, Vol. 15, Page 2507 15 (2023) 2507. https://doi.org/10.3390/POLYM15112507.

[73] C. Shi, X. Hou, D. Zhao, H. Wang, R. Guo, Y. Zhou, Preparation of the bioglass/chitosan-alginate composite scaffolds with high bioactivity and mechanical properties as bone graft materials, J. Mech. Behav. Biomed. Mater. 126 (2022) 105062. https://doi.org/10.1016/J.JMBBM.2021.105062.

[74] B.N. Singh, V. Veeresh, S.P. Mallick, S. Sinha, A. Rastogi, P. Srivastava, Generation of scaffold incorporated with nanobioglass encapsulated in chitosan/chondroitin sulfate complex for bone tissue engineering, Int. J. Biol. Macromol. 153 (2020) 1–16. https://doi.org/10.1016/J.IJBIOMAC.2020.02.173.

[75] S. Kumari, P. Srivastava, A. Mishra, Generation of bioactive porous chitosan/gelatin based scaffold modified with tri-calcium phosphate/nano-bioglass for bone tissue engineering applications, J. Porous Mater. 30 (2023) 1085–1099. https://doi.org/10.1007/S10934-022-01406-Y/METRICS.

[76] V.K. Moses, V. Kandi, S.K.D. Rao, V.K. Moses, V. Kandi, S.K.D. Rao, Minimum Inhibitory

Concentrations of Vancomycin and Daptomycin Against Methicillin-resistant Staphylococcus Aureus Isolated from Various Clinical Specimens: A Study from South India, Cureus 12 (2020) 3883–3886. https://doi.org/10.7759/CUREUS.6749.

[77] G. Wang, J.F. Hindler, K.W. Ward, D.A. Bruckner, Increased vancomycin MICs for Staphylococcus aureus clinical isolates from a university hospital during a 5-year period, J. Clin. Microbiol. 44 (2006) 3883–3886. https://doi.org/10.1128/JCM.01388-06/ASSET/250670E8-3FFA-4F4E-B6F1-C97418FBF9CE/ASSETS/GRAPHIC/ZJM0110668460003.JPEG.

[78] M.J. Rybak, J. Le, T.P. Lodise, D.P. Levine, J.S. Bradley, C. Liu, B.A. Mueller, M.P. Pai, A. Wong-Beringer, J.C. Rotschafer, K.A. Rodvold, H.D. Maples, B.M. Lomaestro, Therapeutic monitoring of vancomycin for serious methicillin-resistant Staphylococcus aureus infections: A revised consensus guideline and review by the American Society of Health-System Pharmacists, the Infectious Diseases Society of America, the Pediatric Infectious Diseases Society, and the Society of Infectious Diseases Pharmacists, Am. J. Heal. Pharm. 77 (2020) 835–864. https://doi.org/10.1093/AJHP/ZXAA036.

[79] A.M. El-Kady, M.M. Farag, A.M.I. El-Rashedi, Bioactive glass nanoparticles designed for multiple deliveries of lithium ions and drugs: Curative and restorative bone treatment, Eur. J. Pharm. Sci. 91 (2016) 243–250. https://doi.org/10.1016/J.EJPS.2016.05.004.

[80] M.Y. Memar, M. Yekani, S. Farajnia, F. Ghadiri Moghaddam, E. Nabizadeh, S. Sharifi, S. Maleki Dizaj, Antibacterial and biofilm-inhibitory effects of vancomycin-loaded mesoporous silica nanoparticles on methicillin-resistant staphylococcus aureus and gram-negative bacteria, Arch. Microbiol. 205 (2023) 1–16. https://doi.org/10.1007/S00203-023-03447-6/METRICS.

[81] T. Cheng, H. Qu, G. Zhang, X. Zhang, Osteogenic and antibacterial properties of vancomycin-laden mesoporous bioglass/PLGA composite scaffolds for bone regeneration in infected bone defects, Artif. Cells, Nanomedicine, Biotechnol. 46 (2018) 1935–1947. https://doi.org/10.1080/21691401.2017.1396997.

[82] S.N. Rahaman, N. Ayyadurai, S.K. Anandasadagopan, Synergistic effect of vancomycin and gallic acid loaded MCM-41 mesoporous silica nanoparticles for septic arthritis management, J. Drug Deliv. Sci. Technol. 82 (2023) 104353. https://doi.org/10.1016/J.JDDST.2023.104353.

[83] T.E. Swanson, X. Cheng, C. Friedrich, Development of chitosan–vancomycin antimicrobial coatings on titanium implants, J. Biomed. Mater. Res. Part A 97A (2011) 167–176. https://doi.org/10.1002/JBM.A.33043.

[84] J. Xu, B. Xu, D. Shou, X. Xia, Y. Hu, Preparation and Evaluation of Vancomycin-Loaded N-trimethyl Chitosan Nanoparticles, Polym. 2015, Vol. 7, Pages 1850-1870 7 (2015) 1850–1870. https://doi.org/10.3390/POLYM7091488.

[85] B. Farasati Far, M.R. Naimi-Jamal, M. Jahanbakhshi, A. Hadizadeh, S. Dehghan, S. Hadizadeh, Enhanced antibacterial activity of porous chitosan-based hydrogels crosslinked with gelatin and metal ions, Sci. Reports 2024 141 14 (2024) 1–15. https://doi.org/10.1038/s41598-024-58174-9.

[86] J. Li, S. Zhuang, Antibacterial activity of chitosan and its derivatives and their interaction mechanism with bacteria: Current state and perspectives, Eur. Polym. J. 138 (2020) 109984. https://doi.org/10.1016/J.EURPOLYMJ.2020.109984.

[87] M.S. Benhabiles, R. Salah, H. Lounici, N. Drouiche, M.F.A. Goosen, N. Mameri, Antibacterial

activity of chitin, chitosan and its oligomers prepared from shrimp shell waste, Food Hydrocoll. 29 (2012) 48–56. https://doi.org/10.1016/J.FOODHYD.2012.02.013.

[88] C. Ardean, C.M. Davidescu, N.S. Nemeş, A. Negrea, M. Ciopec, N. Duteanu, P. Negrea, D. Duda-seiman, V. Musta, Factors Influencing the Antibacterial Activity of Chitosan and Chitosan Modified by Functionalization, Int. J. Mol. Sci. 2021, Vol. 22, Page 7449 22 (2021) 7449. https://doi.org/10.3390/IJMS22147449.

[89] S. Begum, W.E. Johnson, T. Worthington, R.A. Martin, The influence of pH and fluid dynamics on the antibacterial efficacy of 45S5 Bioglass, Biomed. Mater. 11 (2016). https://doi.org/10.1088/1748-6041/11/1/015006.

[90] M. Rismanchian, N. Khodaeian, L. Bahramian, M. Fathi, H. Sadeghi-Aliabadi, In-vitro Comparison of Cytotoxicity of Two Bioactive Glasses in Micropowder and Nanopowder forms, Iran. J. Pharm. Res. IJPR 12 (2013) 437. /pmc/articles/PMC3813266/ (accessed September 18, 2024).

[91] M. Lu, J. Liao, J. Dong, J. Wu, H. Qiu, X. Zhou, J. Li, D. Jiang, T.C. He, Z. Quan, An effective treatment of experimental osteomyelitis using the antimicrobial titanium/silver-containing nHP66 (nano-hydroxyapatite/polyamide-66) nanoscaffold biomaterials, Sci. Reports 2016 61 6 (2016) 1–14. https://doi.org/10.1038/srep39174.

[92] L. Han, Z. Huang, M. Zhu, Y. Zhu, H. Li, Drug-loaded zeolite imidazole framework-8-functionalized bioglass scaffolds with antibacterial activity for bone repair, Ceram. Int. 48 (2022) 6890–6898. https://doi.org/10.1016/J.CERAMINT.2021.11.243.

[93] L.L. Hench, Genetic design of bioactive glass, J. Eur. Ceram. Soc. 29 (2009) 1257–1265. https://doi.org/10.1016/J.JEURCERAMSOC.2008.08.002.

[94] F.E. Ciraldo, E. Boccardi, V. Melli, F. Westhauser, A.R. Boccaccini, Tackling bioactive glass excessive in vitro bioreactivity: Preconditioning approaches for cell culture tests, Acta Biomater. 75 (2018) 3–10. https://doi.org/10.1016/J.ACTBIO.2018.05.019.

[95] A. Hoppe, N.S. Güldal, A.R. Boccaccini, A review of the biological response to ionic dissolution products from bioactive glasses and glass-ceramics, Biomaterials 32 (2011) 2757–2774. https://doi.org/10.1016/J.BIOMATERIALS.2011.01.004.

[96] M. Naeimi, R. Tajedin, F. Farahmandfar, M. Naeimi, M. Monajjemi, Preparation and characterization of vancomycin-loaded chitosan/PVA/PEG hydrogels for wound dressing, Mater. Res. Express 7 (2020) 095401. https://doi.org/10.1088/2053-1591/ABB154.

[97] J. Xu, B. Xu, D. Shou, X. Xia, Y. Hu, Preparation and Evaluation of Vancomycin-Loaded N-trimethyl Chitosan Nanoparticles, Polym. 2015, Vol. 7, Pages 1850-1870 7 (2015) 1850–1870. https://doi.org/10.3390/POLYM7091488.

[98] Q. Zhang, Y. Li, H. Sun, L. Zeng, X. Li, B. Yuan, C. Ning, H. Dong, X. Chen, hMSCs bridging across micro-patterned grooves, RSC Adv. 5 (2015) 47975–47982. https://doi.org/10.1039/C5RA06414G.

[99] P.J. Albert, U.S. Schwarz, Optimizing micropattern geometries for cell shape and migration with genetic algorithms, Integr. Biol. (Camb). 8 (2016) 741–750. https://doi.org/10.1039/C6IB00061D.